IMPROVING THE PERFORMANCE OF LORAWAN IOT SYSTEM

by

Gökçer Yapar

B.S., Computer Engineering, Middle East Technical University, 2015

Submitted to the Institute for Graduate Studies in
Science and Engineering in partial fulfillment of
the requirements for the degree of
Master of Science

Graduate Program in Computer Engineering

Boğaziçi University

2019

ACKNOWLEDGEMENTS

First of all, I would like to thank my thesis supervisor Prof. Tuna Tugcu for his patience, for the opportunities he provided to me, and for his contribution to this thesis. I would also like to thank Orhan Ermis for his valuable comments and ideas. I am also very thankful to Meric Turan for his informative behaviour and his friendship during the thesis process.

I am also very thankful to Zeynep Cinar for her love and smile. She always encourages me for everything by her positive thinking in our stressful situations. Thanks for spending her time to scan the drafts of my thesis and for her helpful comments.

Most important of all, I am very grateful to my parents Necla Yapar and Huseyin Yapar and my brother Oytun Yapar. During my whole life, they always provide unlimited support, encouragement, and tolerance.

ABSTRACT

IMPROVING THE PERFORMANCE OF LORAWAN IOT SYSTEM

One of the technologies developed in LPWAN according to the IoT concept is the LoRaWAN protocol. This protocol works together with LoRa modulation. So far, studies on this protocol included only uplink communication. Moreover, the performance of the pure ALOHA type MAC protocol used in this protocol was not fully observed. Recently, investigations, including downlink communication, have revealed that the pure ALOHA type MAC protocol and downlink traffic have a negative impact on network scaling. A solution is provided to minimize these negative effects in the LoRaWAN protocol. This solution is a scheduling method for synchronizing the gateway with the end devices. In addition, the proposed solution provides two different methods of sending aggregated acknowledgment messages, which are sent to the last devices from the gateway. This proposed solution has been observed to reduce downlink traffic when it is run with various test scenarios and to increase the capacity of the last device to which a gateway can serve. In other words, the proposed solution had a positive contribution to LoRaWAN scaling.

ÖZET

LORAWAN IOT SİSTEMİ'NİN PERFORMANSINI İYİLEŞTİRME

LPWAN içerisinde IoT konseptine uygun olarak geliştirilmiş olan teknolojilerden bir tanesi de LoRaWAN protokolüdür. Bu protokol LoRa modulasyonu ile birlikte çalışmaktadır. Şimdiye kadar bu protokol ile ilgili yapılan çalışmalar sadece yukarı yönlü iletişimi kapsıyordu. Ayrıca, bu protokol içerisinde kullanılan saf ALOHA tipindeki MAC protokolünün performansı tam olarak gözlemlenmiyordu. Son zamanlarda, aşağı yönlü iletişimi de kapsayan araştırmalar saf ALOHA tipindeki MAC protokolünün ve aşağı yonlü trafiğin ağın ölçeklendirmesi üzerinde negatif bir etkisi olduğu sonucunu ortaya çıkarmıştır. Bu negatif etkileri LoRaWAN protokolü içerisinde aza indirgiyebilmek için bir çözüm sunulmuştur. Bu çözüm ağ geçidi ile son cihazların senkronize bir şekilde çalışmasına yarayan bir takvimlendirme metodudur. Ayrıca, önerilen çözüm ağ geçidinden son cihazlara yollanan, aşağı yönde ki trafiği oluşturan, bilgilendirme mesajlarının toplu yollanmasını içeren iki tane de farklı yöntem sunmaktadır. Önerilen çözüm, çeşitli deney senaryolarıyla çalıştırıldığında, aşağı yöndeki trafiği azalttığı ve bir ağ geçidinin hizmet verebileceği son cihaz kapasitesini artırdığı gözlemlenmiştir. Başka bir deyişle, önerilen çözümün LoRaWAN'ın ölçeklendirilmesinde pozitif yönlü bir katkısı olmuştur.

TABLE OF CONTENTS

LIST OF FIGURES

LIST OF TABLES

LIST OF SYMBOLS

B	bandwidth
$Cell_i$	i_{th} cell
ED_i	i_{th} ED
g_i	i_{th} group
G_i	i_{th} super-group
GW_i	i_{th} GW
l_p	p property of the payload
n_i	symbol number of i
p_i	transmission period of i
P_s	probabilty of s
R_i	data rate of i
SF_i	spreading factor i
$slot_i$	i_{th} slot
t_i	time duration of i
T_i	transmission time of the i_{th} group
TOA_i	time-on-air of i
t_i^j	i time duration of j
α_i	i_{th} state

LIST OF ACRONYMS/ABBREVIATIONS

A2S2-LoRaWAN	Aggregated Acknowledgement Slotted Scheduling LoRaWAN
ABP	Activation By Personalisation
ACK	Acknowledgment
AS	Application Server
BEA	Boolean Expression Aggregation
CSS	Chirp Spread Spectrum
DC	Duty Cycle
DL	Downlink
ED	End-Device
ETSI	European Telecommunications Standard Institute
FEC	Forward Error Correction
FSK	Frequency Shift Keying
GW	Gateway
IoT	Internet of Things
ISM	Industrial, Scientific and Medical
LBT	Listen-Before-Talk
LoRa	Long Range
LoRaWAN	Long Range Wide Area Network
LPWAN	Low Power Wide Area Network
MAC	Medium Access Control
NA	Naive Aggregation
NS	Network Server
OTAA	Over-The-Air Activation
PHY	Physical
RF	Radio Frequency
SF	Spreading Factor
UL	Uplink

1. INTRODUCTION

The use of wireless communications became widespread everywhere in routine life. In parallel, the improvements on Internet of Things (IoT) supports and increases the public usage of it. IoT devices and services take the place of monotony human tasks as generating data, sensing information, or maintaining request-based services [1]. According to a prediction of Cisco, there will be 12 billion connected devices until 2020. People will use IoT devices for monitoring purpose [2]. In other words, their traffic mostly contains uplink (UL) data, so they become data generators [3].

From the perspective of the communications, the communication requirements for IoT applications, such as agricultural, industrial, smart city, or smart home, are different [4, 5]. An agricultural application could operate on a communication infrastructure, which supports long-range and low power transmission, concerning conditions of its deployed environments. Additionally, short-range communication, including high energy efficiency, could be a base for smart home application. Thus, there is no single communication model or protocol for all application types. In terms of long-range and low-power applications, Low Power Wide Area Network (LPWAN) technologies are suitable candidates for realizing the applications.

LPWAN technologies mainly focus on scalability, coverage, and energy efficiency. Furthermore, they also work in the Industrial, Scientific and Medical (ISM) bands [6]. Some short-range technologies also operate in the unlicensed ISM bands [7]. Most of the LPWAN technologies could be classified by considering their operating band: wideband or ultra-narrowband. The wideband technologies use a broader bandwidth than required and accept various controlled frequencies to reconstruct data. On the other hand, the ultra-narrowband technologies modulate data within ultra-narrow bands after that applying Digital Signal Processing data reconstruction methods and high-resolution Radio Frequency (RF) crystals for obtaining data [8]. Moreover, each device on the unlicensed ISM bands should comply with regional regulations for supporting multiple protocols as running simultaneously. In Europe, regulations of European

Telecommunications Standard Institute (ETSI) are applied. For example, if a device does not have Listen-Before-Talk (LBT) mechanism, it should limit its communication considering a duty cycle (DC) constraint on its communication subband. LPWAN technologies generally have a star topology, so that they directly talk with their base-stations. Moreover, some LPWAN technologies have limitations on their downlink (DL) for generating minimal DL traffic. In terms of applications, LPWAN is not feasible for applications requiring high throughput, high energy consumption, and short distance communication. For supporting the applications requiring low throughput, low energy consumption and long distance communication, Long Range (LoRa)/Long Range Wide Area Network (LoRaWAN), Sigfox, Weightless-P, NB-IoT, EC-GSM-IoT and RPMA of Ingenu could be used as LPWAN technologies [9].

Sigfox, which is an ALOHA-based ultra narrowband technology, operates on sub-GHz ISM bands. Also, Sigfox is not a fully bi-directional technology [10]. Therefore, in Sigfox there are subscription types based on the maximum number of bytes per day for UL and the maximum number of packets for UL and DL, instead of complying with the DC restriction defined in the regional regulations. NB-IoT and EC-GSM-IoT are cellular IoT-based LPWAN technologies [10], which operate on licensed bands and deal with the regional regulations on DC constraints. RPMA of Ingenu uses spread spectrum techniques, similar to LoRa, for modulation. However, it operates in the 2.4 GHz band, as opposed to LoRa, so that its range is shorter. Furthermore, ETSI has not defined DC regulations for the 2.4 GHz band in Europe.

1.1. Motivation

LoRaWAN operates in sub-GHz ISM bands [11]. Thus, LoRaWAN devices have to comply with wireless communication policies defined by ETSI, for Europe, enforcing restrictions on its transmission on the unlicensed bands. Since it lacks LBT mechanism, a LoRa device can transmit for 36 seconds per hour in a subband at most with 1% DC constraint. This is valid also for DL. Although IoT devices are positioned as data generators, LoRaWAN devices should be as effective as the RPMA acknowledgment (ACK) mechanism at DL communication for improving the reliability of applications.

Due to collisions or DC constraints, ACK messages could not be sent to LoRaWAN devices that results in the retransmission of the same messages. Consequently, the collision in the network increases with growing UL traffic. Since LoRaWAN devices make transmission at a frequency band by applying ALOHA-based approach while complying with the regional DC regulations [12]. Also, it is clearly seen that DL traffic negatively affects UL traffic indirectly when looking for former explanations. When UL traffic is increasing, the scalability of the LoRaWAN network also is negatively affected. As a result, LoRaWAN network cannot handle the more devices anymore. The problem is the use of ALOHA-based approach in LoRaWAN instead of DC friendly medium access approach. Furthermore, the problem could be seen in an application requiring ACK messages for End-Devices (EDs). The problem adversely affects the network scalability and network traffic.

1.2. Contributions of This Thesis

In this thesis, the following contributions are proposed for solving the scalability problem of the LoRaWAN:

- We propose DC-friendly time-slotted ALOHA based LoRaWAN scheduling for improving network scalability and decreasing UL message traffic. It is called Aggregated Acknowledgment Slotted Scheduling LoRaWAN (A2S2-LoRaWAN).
- We propose two methods used in A2S2-LoRaWAN to decrease DL message traffic by aggregating ACK messages. These are called Naive Aggregation (NA) and Boolean Expression Aggregation (BEA).
- We derive a mathematical models for A2S2-LoRaWAN scheduling model. It is used for validating the proposed system performance.
- We define simulation scenarios considering the increasing number of devices in the network, increasing the load of message payload sent from ED to Gateway (GW) and changing the Spreading Factor (SF) based distribution of the EDs inside the network.

1.3. Organization of The Thesis

The rest of the thesis is organized as follows: In Chapter 2, we give an overview of LoRaWAN and LoRa. In Chapter 3, we present the previous works in tge literature related to LoRaWAN. These works are about DL traffic effects, system scheduling models, and mathematical models for LoRaWAN. In Chapter 4, the proposed method A2S2-LoRaWAN is presented. In Chapter 5, we show results of the proposed scheduling model, its corresponding mathematical model, and LoRaWAN according to the defined scenarios. In Chapter 6, we conclude the thesis and define our future research directions.

2. OVERVIEW OF LONG RANGE WIDE AREA NETWORK

This chapter provides background information about LoRaWAN by first introducing the general network information about LoRaWAN and network topology. Then, device types in LoRaWAN are defined in the second section. Consequently, Physical (PHY) and Medium Access Control (MAC) layer information of LoRaWAN is given in the third and fourth sections. Lastly, some limitations described for LoRaWAN are supplied in the fifth section.

2.1. Network Topology

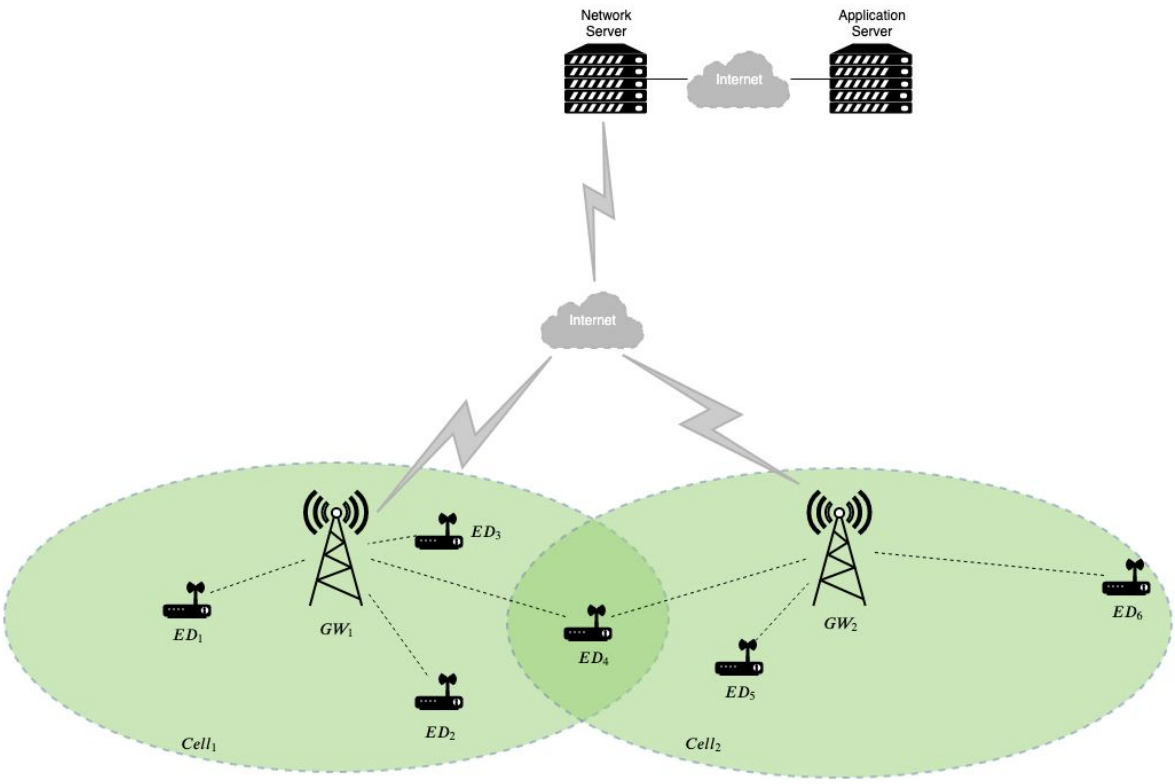

Figure 2.1. LoRaWAN network topology, $ED_{[1-4]}$ in $Cell_1$ can make transmission to Network Server over GW_1, and $ED_{[4-6]}$ in $Cell_2$ can make transmission to Network Server over GW_2.

LoRaWAN networks are composed of three main network components: EDs, GWs and centralized Network Server (NS). A LoRaWAN network is laid out in a start-of-stars topology (Figure 2.1). Moreover, there is not a direct connection between the EDs and the NS. The communication is established over the GW, which relays the message of the ED to NS through a reliable and high throughput link indirectly. In addition, the transmissions on the wireless communication channel between the ED and the GW are modulated by using LoRa or Frequency Shift Keying (FSK) modulation. In the topology represented in Figure 2.1, there is no rule for ED that it should send its message to an attached GW, because there is no terminal attachment for the network. So, EDs can make their transmissions to available GWs; ED_4 in Figure 2.1 can send its message to GW_1 and GW_2. After receiving a message from the ED, each GW forwards it to a centralized NS that is responsible for selecting the best GW to transmit DL communications to the ED and filtering duplicate messages. For the purpose of maximizing the resilience of the network to interference and to make it robust against distortions in the wireless channel, multiple logical channels are determined for the entire network. Also, EDs are expected to choose a channel in a pseudo-random fashion.

To get an ED connected to LoRaWAN, the ED has to first register to the network (Figure 2.2). There are two types of registration methods in LoRaWAN: Over-The-Air Activation (OTAA) and Activation By Personalisation (ABP). In the ABP method, the ED is already known by the NS so there is no need for any extra join request from the ED to the NS, as opposed to the OTAA method. After successfully finishing the registration operation, the ED can transmit its message under the rules of LoRaWAN. α_1 and α_2 states of ED_1 are shown in Figure 2.2. According to the example, in the state α_1, ED chooses OTAA method for registering to LoRaWAN. After sending a join request to the NS, if the NS verifies the request is valid, then it sends a join-accept response, which contains the ED address and a certificate for secure communication between the ED and the NS, to the ED. After registering into the NS, the ED can send its data to the Application Server (AS) over the NS, as in the state α_2. If the data sent by the ED is of confirmed message type, the NS sends an ACK to the ED.

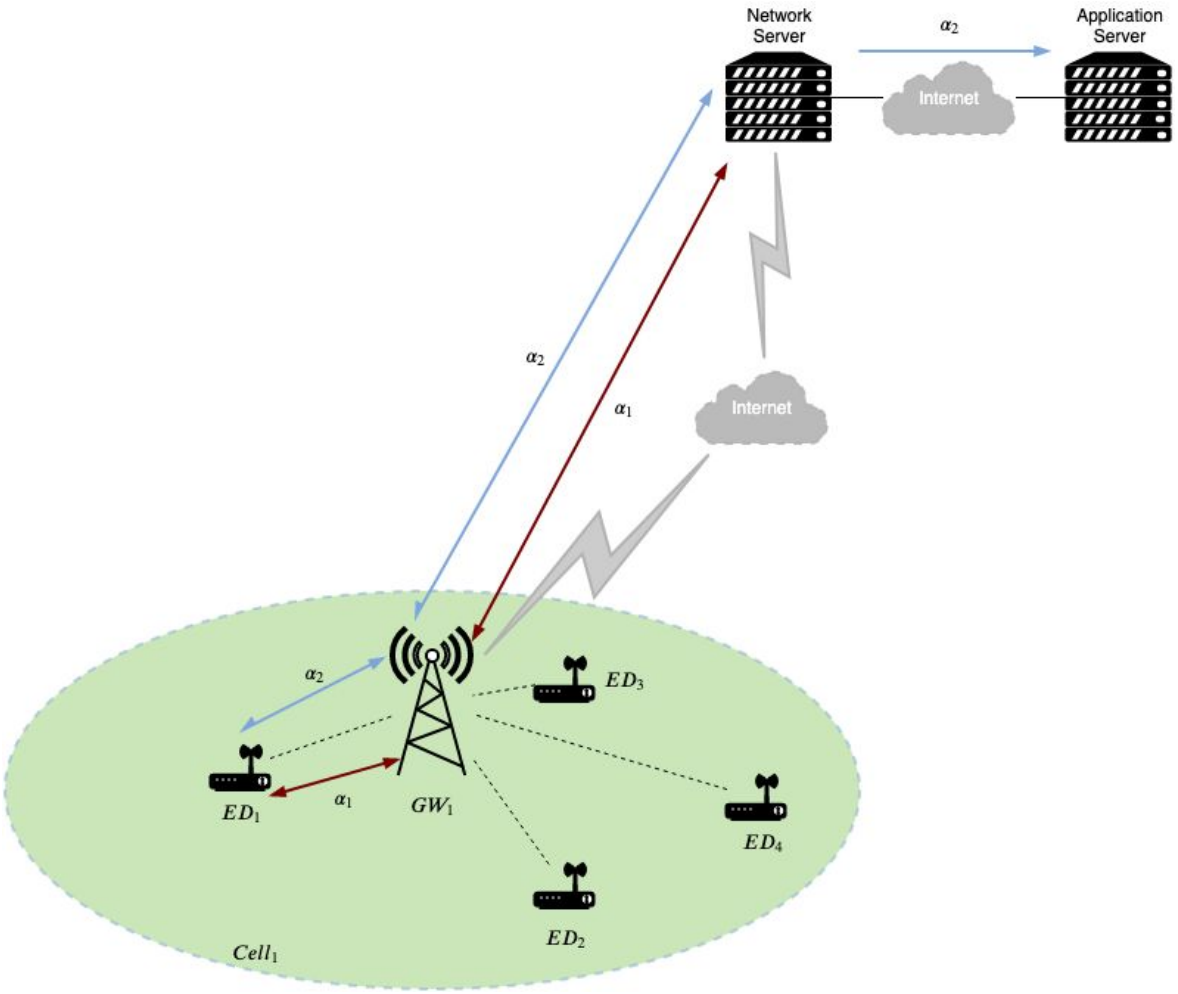

Figure 2.2. Lifecycle of ED_1 in $Cell_1$ at LoRaWAN network

In Figure 2.3, LoRaWAN protocol stack is deployed into the EDs and the NS as the MAC and PHY layers. However, GW is not aware of LoRaWAN MAC protocol, and its only task is to deliver the data between the ED and the NS.

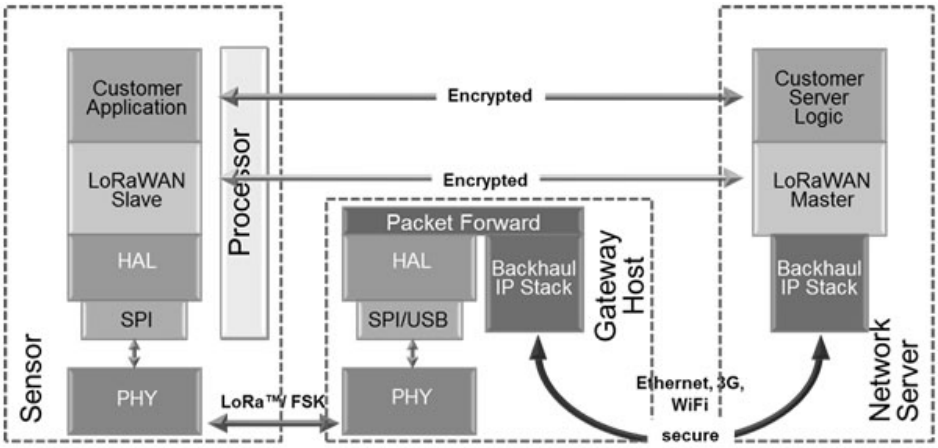

Figure 2.3. LoRaWAN Protocol Stack

2.2. Device Types

According to LoRaWAN specifications, there are three types of devices for the usecases of the EDs: Class A, Class B, and Class C, which are mainly distinguished with respect to their different behavior against power consumption and transmission schedule [13]. Enforced by the standard, all LoRaWAN EDs must implement Class A features, and the implementation of the other two classes is optional. In this thesis, we focus solely on Class A devices.

2.2.1. Class A

Transmission schedule is based on the communication needs of the ED whose communication channel is bi-directional. An ED of Class A opens its receive window after transmitting the message to GW. DL communication is not initialized by the NS; in other words, it could be active after a UL communication initiated by the ED. In addition, they access the medium by using a pure ALOHA type of protocol.

To detail the behavior of Class A devices when they are in communication with the GW, let's first define the retransmission and receive window processes [14].

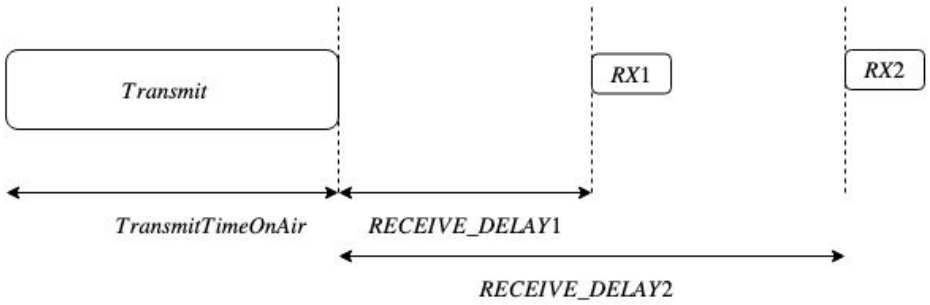

Figure 2.4. LoRaWAN Receive Window

In Figure 2.4, firstly, as specified in the LoRaWAN protocol, two short receive windows must be opened only slightly after the end of the UL communication. The receive window takes the end of the transmission as a reference point to determe its start time. The first receive window, RX1, operates at specific a frequency band and data rate, which is a function of the frequency and the data rate used for the UL. RX1 is opened for listening to DL transmission RECEIVE-DELAY1 seconds after the end of the UL modulation. The relationship between the data rates of UL and DL at RX1 slots is region specific. By default, the first receive window data rate is identical to the data rate of the last UL. Moreover, the second receive window, RX2, utilizes a fixed configurable frequency band and data rate, which is opened RECEIVE-DELAY2 seconds after the end of the UL modulation. The frequency band and data rate applied can be changed by MAC commands. The default frequency and data rate to use are region specific. In addition, an ED cannot send a new message through the UL channel before its first or second receive windows of the previous transmission have taken a DL message, or the second receive window of the previous transmission has expired.

Secondly, as stated in LoRaWAN protocol specification, DL and UL frames can be confirmed or unconfirmed frames. In other words,the ED should be acknowledged after transmitting a confirmed message by the GW for verifying the communication status of the sent message. On the other hand, an unconfirmed message sent from the

ED to the GW does not need to follow this communication process. In DL frames, unconfirmed and confirmed frames use the same frame counter value so that they shall not be retransmitted. However, if the NS is notified when the ACK is not received by the ED, then it may choose to retransmit the confirmed frame. In UL frames, UL retransmissions are controlled by NbTrans, which is a configurable parameter in a MAC command and is an upper limit for retransmissions so that retransmissions continue until reaching the upper limit of retranmissions. Furthermore, retransmissions may not occur until both RX1 and RX2 receive windows have expired. Besides, the device ceases retransmitting a frame upon the reception of a frame in either the RX1 or the RX2 window.

2.2.2. Class B

EDs of Class B provide extra scheduled receive windows to EDs of Class A random receive windows. To open its extra receive window at the scheduled time, the ED gets a time synchronized beacon from the GW. After getting the beacon, it schedules its extra receive window for listening to DL transmissions [14].

2.2.3. Class C

EDs of Class C have nearly continuously open receive windows, which are closed only due to bidirectional communication. Power consumption of the Class C type ED is more than that of Class A or Class B. However, they provide the lowest latency in communication between the NS and the ED [14].

2.3. PHY Layer

LoRa is a modulation technique developed and patented by Semtech. It is not an open source technology like LoRaWAN, so there is not a detailed paper about LoRa, providing the design details of LoRa. However, one can be informed about LoRa by reading LoRa chip specifications provided by Semtech or deduce insights from the reverse engineering results [15]. In addition, LoRa uses a spread spectrum technique

called Chirp Spread Spectrum (CSS) and Forward Error Correction (FEC).

2.3.1. Spreading Factor

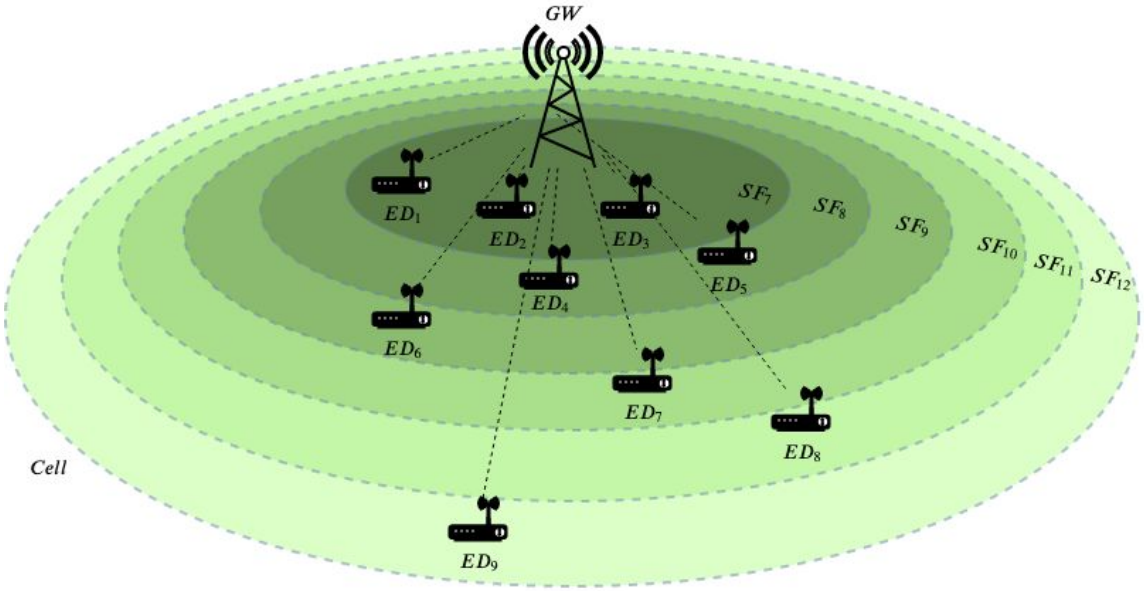

Figure 2.5. LoRaWAN SF example in the *Cell* of the *GW*. $ED_{[1-3]}$ are SF_7, $ED_{[4-5]}$ are SF_8, ED_6 is SF_9, ED_7 is SF_{10}, ED_8 is SF_{11}, and ED_9 is SF_{12}.

In Figure 2.5, EDs in the inner circle of the *Cell* communicate with the *GW* using SF_7, and the ED in the outer circle of the *Cell* transmits its message to the *GW* using SF_{12}. In other words, SFs are increasing when the distance between the ED and the GW is increasing. Thus, time-on-air of ED messages with the same payload from the inner circle to outer circle is increasing since a symbol is encoded with 7 bits for SF_7 and 12 bits for SF_{12}. In addition, different SFs are orthogonal to each other so that there is no collision when EDs have different SFs transmitting messages to the *GW* simultaneously [16].

2.3.2. Chirp Spread Spectrum

CSS is a modulation technique from the spread spectrum modulation family [17]. It uses wideband linear frequency modulated chirp pulses for encoding data. It was designed for radar use in the 1940s. Traditionally used in some applications that

require secure communication feature, the usage of CSS in some data communications applications was increasing in the past years, owing to its low transmission power requirements and its robustness against distortions in the communication channel, such as Doppler effect, multipath fading, and in-band jamming interferences.

LoRa modulation depends on the bandwidth of the channel, the SF, and the coding rate of information because of the fact that these parameters affect the bit rate of the transmission and symbol duration. CSS modulation uses chirp signals for encoding data by increasing or decreasing its frequency. Moreover, there are 2^{SF} possibilities for selecting the frequency offset of the chirp, called as a symbol in LoRa, by the cyclical shift between the minimum and maximum values of the frequency. In addition, each frequency offset of the symbol corresponds to a different chip value, so 2^{SF} chip values per symbol are possible, which could be encoded as the number of SF bits. Also, we know that the chip rate is equal to bandwidth of the modulation. Thus, we can define the symbol duration as

$$t_{symbol} = \frac{2^{SF}}{B}. \tag{2.1}$$

Furthermore, we know the number of bits per symbol for encoding data, so we can define data rate or bit rate as

$$R_{bit} = \frac{SF}{t_{symbol}}. \tag{2.2}$$

2.3.3. PHY Frame Format

PHY frame formats are classified as explicit and implicit mode frame. For explicit mode PHY frame, the frame format includes a preamble, a PHY header, a PHY header CRC, PHY payload, and optional CRC fields. The PHY frame format can be represented as in Figure 2.6 or Figure 2.7.

In Figure 2.6, where the horizontal axis is the time and the vertical axis is the frequency, the spectrogram representation of a LoRa packet sample is given. From the left side to the right side of the spectrogram, three different patterns of lines are remarkable. However, the spectrogram consists of a preamble and a PHY frame. The preamble consists of constant number up-chirps; 2 up-chirps for sync word then 2.25 down-chirps, so the preamble has minimum 4.25 chirps or symbols [18]. After sending the preamble, the rest of the PHY frame is transmitted as up-chirp with frequency jumps. From the perspective of Figure 2.6, first 5 lines (up-chirps) and 2.25 lines (down-chirps) represent the preamble, and the preamble is followed by 8 lines (up-chirps), the PHY frame.

Figure 2.6. Spectrogram of LoRa

On the other side, time-on-air can be calculated by Equation 2.3.

$$TOA_{packet} = t_{preamble} + t_{payload} \tag{2.3}$$

The time-on-air of the packet TOA_{packet} is equal to the summation of $t_{preamble}$ and $t_{payload}$ durations. Preamble duration can be calculated by Equation 2.4.

$$t_{preamble} = (n_{preamble} + 4.25) \cdot t_{symbol} \tag{2.4}$$

$n_{preamble}$ is the programmed preamble length and t_{symbol} is the symbol duration, which is calculated by Equation 2.1. In addition, the payload duration can be calculated by Equation 2.5.

$$t_{payload} = n_{payload} \cdot t_{symbol} \tag{2.5}$$

The number of payload symbols, $n_{payload}$, can be calculated by using Equation 2.6, where PL is the payload length in bytes, SF is LoRa SF changing from 7 to 12, H is the packet header (0 when the header is enabled and 1 when no header is present), DE is the data rate optimizer (1 when enabled, 0 otherwise), and CR is LoRa coding rate (1: 4/5, 2: 4/6, 3: 4/7, 4: 4/8).

$$n_{payload} = 8 + max\left(ceil\left[\frac{8PL - 4SF + 28 + 16CRC - 20H}{4(SF - 2DE)}\right](CR + 4), 0\right) \tag{2.6}$$

2.4. MAC Layer

LoRaWAN is the MAC protocol for LPWAN and runs on the LoRa. LoRaWAN brings the advantages of consuming low power and transmitting a message to a long-range area for EDs. As mentioned earlier, there are three classes of the protocol. All LoRaWAN classes communicate bi-directionally. However, there are differences in their power consumption and message transmission schedule. The messages are transmitted in UL and DL directions.

2.4.1. MAC Message Format

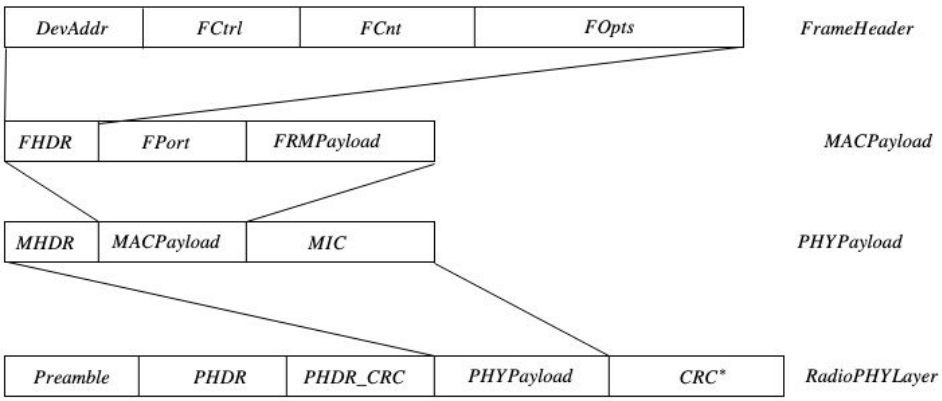

Figure 2.7. LoRa message formats

From the perspective of the Radio PHY Layer, UL and DL PYH frame structures show differences in terms of the existance of CRC field in the frame structure. Additionally, in Figure 2.7, PHY payload is divided into three parts as a single-octet MAC header, a MAC payload, and a 4-octet message integrity code. Firstly, after inspecting the MAC header, the header is used for carrying information about the version of the standard used by the device and about the message type. In particular, expressing the details of the message types is necessary. There are data, join and proprietary messages. A data message could be a UL message or a DL message. Besides, a data message is defined as a confirmed message or an unconfirmed message. Furthermore, join messages are sent by the ED as a first communication for registering to a network. Secondly, MAC payload consists of a frame header, a frame port, and a frame pay-

load. In the frame header, the header contains an ED address, a frame control octet, a 2-octet frame counter, and up to 15 octets of frame options used to transport MAC commands. Lastly, MIC is used for protecting the integrity of the message.

2.4.2. MAC Commands

MAC commands are not visible at the application layer. Besides, they are exchanged between the NS and MAC layer of the ED. In addition, as shown in Table 2.1, MAC commands provide the flexibility of remotely configuring the behavior of the LoRaWAN components in the network for network administration. Some features of the MAC commands are described in Table 2.1. In addition to Table 2.1, there are other 128 command identifiers, which are reserved for proprietary network command extensions.

Table 2.1. Feature of some MAC Commands

Feature	**MAC Commands**	**Detail**
Configuring Receive Window	RXTimingSetupReq RXTimingSetupAns RXParamSetupReq RXParamSetupAns	Configuring delay of receive windows and its data rates and frequency channel according to the specification
Getting Device Status	DevStatusReq DevStatusAns	Getting status of the ED contains its battery level and its demodulation margin
Link Checking	LinkCheckReq LinkCheckAns	Giving information about the channel quality
Configuring DC	DutyCycleReq DutyCycleAns	Configuring device's aggregated transmission time

2.5. Limitations

LoRaWAN operates on ISM bands, which are unlicensed and free to use subject to compliance with the regulations on the communication channel [19]. Furthermore, the details of the regulations may vary between regions, based on regional regulations. The regional regulations affect the maximum payload size, receive windows size, the size of the preamble, supported SFs, and used channel frequencies. According to the specifications, LoRaWAN devices can be deployed in the three regions China, Europe, and the US [20]. The used frequency bands in ISM are shown in the Table 2.2.

Table 2.2. LoRaWAN frequency bands for the different regions

Region	**Frequency Band**
China	779-787 MHz
EU	863-870 MHz, 443 MHz
US	902-928 MHz

According to ETSI [7], which is one of the organisms for regulating spectrum usage in EU, if a device does not use LBT policy when accessing the medium in ISM bands, the device should comply with the DC regulations on the accessed sub-band. Also, the specification requires a per sub-band DC limitation for a device, as shown in Table 2.3. When a message is sent in a selected sub-band, TOA of the message is stored for this sub-band. The device cannot transmit a new message on the sub-band for a duration defined in seconds. After passing the time-off seconds duration, the device can make a transmission on the same sub-band. However, in the time-off duration, the device can transmit its message only on another sub-band. If all sub-bands are unavailable, the device has to wait before any further transmission. For example, if an ED has just transmitted a 1 s long frame on one default channel in a sub-band (DC is 1%). Thus, this whole sub-band (868 – 868.6) will be unavailable for 99% of the time.

Table 2.3. ETSI DC per subband

Frequencies Boundry	**DC**	**Subband**
865-868 MHz	%1	g
865-870 MHz	%0.1	g
868-868.6 MHz	%1	g1
868.7-869.2 MHz	%0.1	g2
869.4-869.65 MHz	%10	g3
869.7-870 MHz	%1	g4

$$t_{off} = \frac{TOA_{packet}}{DC} - TOA_{packet}. \tag{2.7}$$

The RXTimingSetupReq command is a MAC command in the protocol. The command allows configuring the delay between the end of the UL transmission and the opening of the first receiving slot. The second reception slot opens one second after the first receiving slot. The delay value is an integer and it could be set in a range of one to 15 seconds [21].

Table 2.4. Maximum MAC payload

Data Rate	**Configuration**	**Maximum MAC Payload**
DR0	LoRa: SF12 / 125 kHz	59 byte
DR1	LoRa: SF11 / 125 kHz	59 byte
DR2	LoRa: SF10 / 125 kHz	59 byte
DR3	LoRa: SF9 / 125 kHz	123 byte
DR4	LoRa: SF8 / 125 kHz	250 byte
DR5	LoRa: SF7 / 125 kHz	250 byte

Besides, maximum MAC payload size of the frame varies according to the data

rate of the device [22].

3. LITERATURE SURVEY

A basic performance criterion for LoRaWAN networks is scalability, which is a measure of the number of EDs supported. The performance metric could be related to DL traffic effects on the UL traffic and the medium access protocol working on LoRaWAN.

Scalability of the LoRaWAN network has been studied in the literature. These works inspect the performance metric without considering DL message traffic effects on the UL message traffic. On the other hand, there are other researches, which include DL message effects on the network performance.

LoRaWAN utilizes pure ALOHA type medium access protocol to transmit on a channel [23]. Moreover, EDs select the channels for transmission in a random manner, so there is no scheduling between the devices in a LoRaWAN network. However, there are some works on proposed scheduling mechanisms, which point out the effects of scheduling on network performance.

3.1. Studies on DL Traffic

In [24], Pop *et al.* focus on bidirectional communication with LoRa and LoRaWAN technologies. Besides, LoRaWANSim, which is an extended version of LoRaSim, is implemented with additional features with respect to other LoRa and LoRaWAN simulators for measuring network performance under realistic scenarios. Additionally, the authors suggest that the DL traffic can have adverse effects on the UL throughput. Also, retransmissions result in increasing energy consumptions and collisions in the network. LoRaWANSim realizes DL traffic, DC regulations, collision model, and retransmission procedure in LoRaWAN. According to the retransmission procedure in LoRaWANSim, the retransmission may happen when the transmission collides with other transmission or the GW is unavailable to send an ACK due to DC restriction. Besides, LoRaWANSim in the considered testcases runs with a network

topology that contains between 100 and 5000 EDs. After running LoRaWANSim, the authors make some important deductions:

- DC restriction on the GW and collisions result in unreliable DL in LoRaWAN.
- Retransmissions cause a significant drop in network goodput.
- In LoRaWAN networks with large number of nodes requiring ACK does not scale.

In [25], the effect of the DL traffic on the performance of the UL traffic for LoRaWAN operating at 868 MHz band is investigated empirically. Also, the authors emphasize that the influence of DL transmission on the UL traffic should be considered when planning a LoRaWAN network. The experiment setup contains ten devices with various test cases. After realizing the scenarios, some significant results are gathered from the measurements:

- A LoRaWAN GW is allowed limited DL transmissions due to DC regulations on the DL channels.
- The devices transmitting with low data rates cause an increase in the packet error rate since the longer on-air time increases the probability of collision.
- The first receive window in LoRaWAN uses the same SF and the same frequency channel as the previous UL transmission so there may be a collision with another UL message using the same channel during DL transmission. On the other hand, the second receive window is opened in a pre-defined channel and uses a pre-specified SF. However, a collision on the second receive window is possible since the frequency plan of LoRaWAN does not avoid selecting the same channel for UL communication of another device in the second receive window.

According to these findings, Mikhaylov *et al.* in [25] make some recommendations, which are reducing consequences of the interferences between DL traffic and UL traffic, to increase network performance:

- After preventing the use of the first receive window for DL, the second receive window can be configured for operating on a dedicated channel.

- LBT mechanism can be added to the GW and the ED.
- ED density of the GW can be increased.
- The receive and transmit chains at the GW could be separated physically. Moreover, the GW can use the different antennas for receive and transmit chains.

In [26], the confirmed message feature of the LoRaWAN results in increasing DL transmissions. As a result of the reckless use of this feature, sharp decreases may be observed in the network performance for large scale deployments. The findings in [26] show that the use of the confirmed message in LoRaWAN affects the network capacity and the reliability of the unconfirmed UL traffic because of the DC constraints on the GW and UL/DL packet collisions. To analyze the LoRaWAN performance, NetworkSimulator-3 LoRaWAN module is implemented by the authors in [26]. Furthermore, the simulator is realized as follows:

- Semtech's SX1301 chip, which can only decode eight signals simultaneously, is realized.
- Retransmission is also included.
- The GW transmits only once, in other words, it can transmit on either the first receive window or the second receive window. Besides, it gives priority to the first receive window.
- DL traffic can preempt any UL traffic at the GW, so transmitting ACKs has higher priority over UL transmissions at the GW.
- DC limitation is reflected in the GW communication mechanism as aborting ACK transmission when the GW is in the time-off duration.

The simulator implements a single GW, which is circled by N EDs uniformly distributed in a circular area. Also, it considers confirmed traffic and unconfirmed traffic. After running on test cases, consequences of the collisions and DC restrictions are reflected. On the other side, some recommendations are given for the issues caused by DC restrictions:

- Applying LBT mechanism at the GW.

- Applying DL scheduling, which is controlled by the NS.

3.2. Studies on Scheduling

In [27], Reynders *et al.* propose a new MAC layer, which is called RS-LoRa, to increase the reliability and the scalability of LoRa. In detail, the main contribution of the proposed MAC layer is a two-step lightweight scheduling. First of all, the nodes are scheduled in a coarse-grained manner by a GW by dynamically determining the permitted transmission powers and SFs on each channel. Lastly, nodes make a decision about describing their own transmission power, SF, transmission time, and transmission channel by selecting allowed transmission power and SF list, which is created in the first step. In addition, for realizing an integration between the first and the second steps, the sytem model needs a scheduling model. In the system model, nodes are separated within different groups, and through each group, nodes use similar transmission power to mitigate the capture effect. In other words, the whole band is divided into one synchronous DL channel and several asynchronous UL/DL channels. Furthermore, there are frames, which have the same structure and duration, consisting of subframes. In detail, a subframe starts with a beacon, transmitted by the GW, followed by UL/DL slots. Also, the nodes are directed to choose different SFs to improve reliability and scalability. After realizing the proposed MAC layer in NetworkSimulator-3, one cell scenario with 1000 nodes is simulated. The simulation result shows that RS-LoRa reduces the packet error ratio of LoRaWAN by nearly 20%. On the other hand, the system model of the solution could be improved by considering the DC restriction on the GW for avoiding retransmission and accessing the resource in the subframe could be in a slotted manner for increasing the network reliability.

In [28], Haxhibeqiri *et al.* implement an on-demand scheduling approach, in which the nodes demand time slots from the GW. In detail, the GW sends selected time slot indices encoded in a bloom filter, a probabilistic data structure, to the nodes. By using the data structure, it minimizes the DL traffic. Hence, the effects of the DC on the DL is decreased. In addition, it does not eliminate the collisions because of the fact that the probabilistic data structure can have false positives. After running test

scenarios with the solution, 7% and 30% increases in packet delivery ratio for SF7 and SF12 occur at Class A of LoRaWAN.

In [29], two offline algorithms about allocating SFs mechanism are developed for minimizing the total time of data collection at the nodes. These algorithms respect DC limitations. The algorithms are Global Allocation and Light Allocation. For creating a base to the algorithms, a system model is designed for representing time slots and scheduled frames, which are two-dimension arrays with six rows and a row for each SF. Furthermore, the frame structure is used by the algorithms for finding the best time slot location per transmission. Also, in a row, transmissions for the same SF are accommodated once after the another while the transmissions of different SFs can happen concurrently. Thus, the total data collection time is minimized. Global Allocation schedules the whole operation at once. In contrast to the Global Allocation, Light Allocation algorithm generates a recurrent schedule consisting of repeated frames. After running test cases with the proposed solutions, some improvements are observed. However, the test scenarios should be run with more than 1000 nodes and run with packet size supported by all SF device. The solution could be redesigned by considering confirmed messages.

3.3. Other Related Studies

In [30], the main contribution is a mathematical model, which analyzes the packet error rate behavior against offered load change in the LoRaWAN network. Furthermore, the authors describe a collision in the model as two frames colliding when they transmit with the same data rate on the same channel at the same time. Besides, the model structure is based on several assumptions:

- EDs generate the traffic based on Poisson process.
- ACKs carry no frame payload.
- A transmission is counted as successful if there is no collision with any transmission or ACK is received by the ED.
- The GW ignores ACK transmission if it is receiving a message.

The model is the first mathematical model, which includes retransmission and ACK features of the LoRaWAN. However, it does not consider DC limitations.

In [31], the proposed mathematical model makes it feasible to predict the probability of success for the packets in LoRaWAN with the presence of the bi-directional traffic: UL and DL transmissions. The proposed mathematical model realizes the critical features of the LoRa chipset and LoRaWAN standard. Besides, the model structure is based on some assumptions:

- The network is located in an open-air scenario, which contains only one GW, so there is only path loss propagation model.
- EDs generate confirmed data packets with the Poisson process as network traffic. Besides, lost packets, which are unconfirmed, are not retransmitted.
- SF orthogonality is perfect, so the collisions only happen between frames applying the same SF.
- Giving priority transmission or reception at the GW is configurable.
- DC limitations at the GW is configurable.

Additionally, in real life, the GW does not make transmission and reception simultaneously. Also, retransmission should be considered by the model. However, the model does not contain the retransmissions.

4. AGGREGATED ACKNOWLEDGEMENT SLOTTED SCHEDULING

In the first section, we discuss the neutralizing effects of the ALOHA-based MAC protocol in LoRaWAN. Later, the system model and the system design of the proposed A2S2-LoRaWAN are provided. In the last section, the mathematical model derived for the A2S2-LoRaWAN is given.

4.1. Problem Definition

LoRaWAN's scalability problem is due to the negative impact of DL on the UL [26]. This problem is more likely to occur when the number of sent confirmed messages is higher than the number of sent unconfirmed messages because DL is correlated to ACK messages. The main reason for this problem is the ALOHA type MAC protocol used by LoRaWAN and the DC restrictions on DL [25]. In other words, not using a DC-friendly MAC protocol in LoRaWAN returns as a problem for the network scalability.

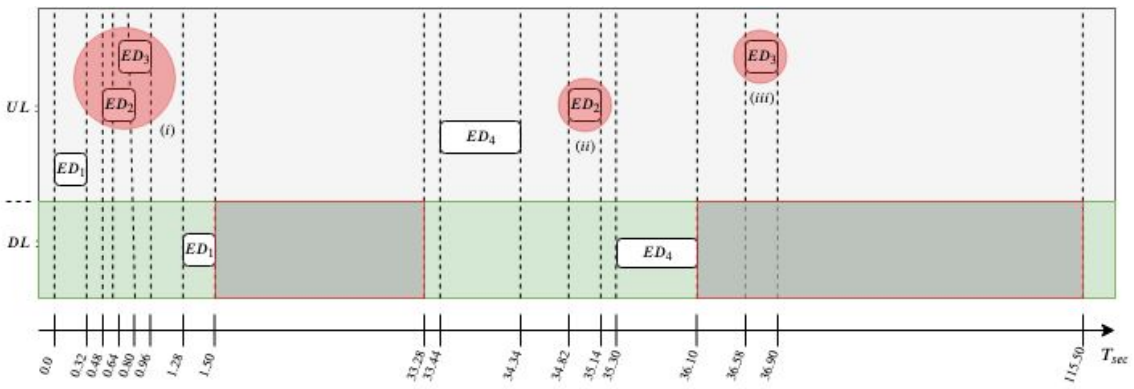

Figure 4.1. Example of failed transmission cases showing UL traffic and DL traffic. $ED_{[1-3]}$ have the same SF, and ED_4 has a different SF from other EDs.

In Figure 4.1, UL traffic and DL traffic are simulated by considering LoRaWAN ALOHA-type MAC protocol. In UL traffic, $ED_{[1-4]}$ transmit their messages to the GW. In DL traffic, with respect to the transmission status of the EDs in the UL, the

GW sends ACK messages to ED_1, between 1.28 and 1.50 seconds, and ED_4, between 35.30 and 36.10 seconds. After transmitting the ACK messages, the GW returns to passive state between $1.50 - 33.28 seconds$ and $36.10 - 115.50 seconds$ with respect to the DC constraints on the DL. Besides, there are three failure transmission cases: (i), (ii), and (iii).

- In case (i), ED_2 and ED_3 with the same SF transmit their messages on the same channel simultaneously, which results in a collision. Consequently, the EDs make retransmissions, which cause a large drop in network goodput [24]. Also, increasing the number of EDs inside the coverage area of the GW causes an increase in the number of collisions between transmissions, which makes it impossible to scale up the network. The reason is that the EDs randomly access the medium by using ALOHA protocol as ED_2 and ED_3.
- In case (ii), ED_2 transmits its message without any collisions. The GW sends ACK message to ED_4, then returns to its transmission state to the passive state due to the DC constraints on DL. Therefore, the GW is not suitable for sending an ACK message to ED_2 during the GW passive state [26]. Consequently, ED_2 does not receive any ACK messages from the GW, so it will make a retransmission, which negatively affects the network scalability again since there is no synchronization between ED_2 and the GW.
- In case (iii), ED_3 transmits its message without any collisions. However, it sends the message to the GW during the passive transmission state and opens its receive window during the passive state of the GW. So, ED_3 does not receive any ACK message, similar to case (ii). Same consequences as in case (ii) are valid for case (iii).

To sum up, the main problems for the network scalability are the existence of unsynchronized transmission between the ED and the GW, and using pure ALOHA-type MAC protocol in LoRaWAN.

4.2. System Design

The system design of the A2S2-LoRaWAN can be explained in three stages: the system model, the system scheduling, and aggregated acknowledgment.

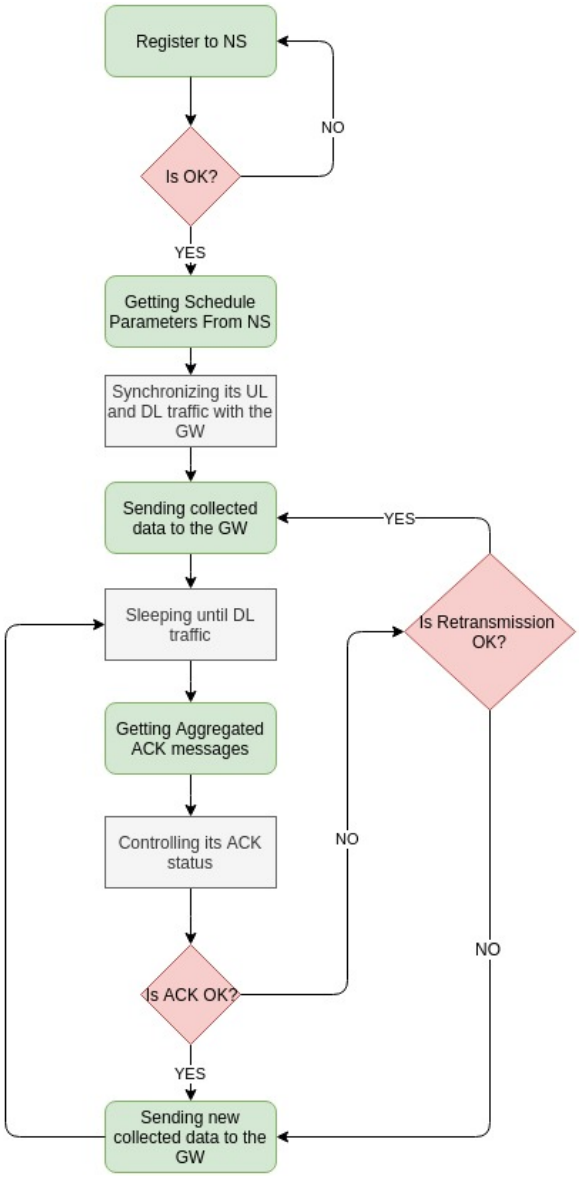

Figure 4.2. An ED lifecycle in the A2S2-LoRaWAN solution as a state diagram.

In Figure 4.2, an ED firstly registers to the NS, then sends a request to get scheduling parameters. After getting the parameters, ED synchronizes its UL traffic and DL traffic.

4.2.1. System Model

In A2S2-LoRaWAN, the entire available channel is divided into repetitive frames, which are called super-group, with a duration of t_G. Each SF has its own super-group overlapping in time with the super-groups of the other SFs. Each super-group consists of several groups.

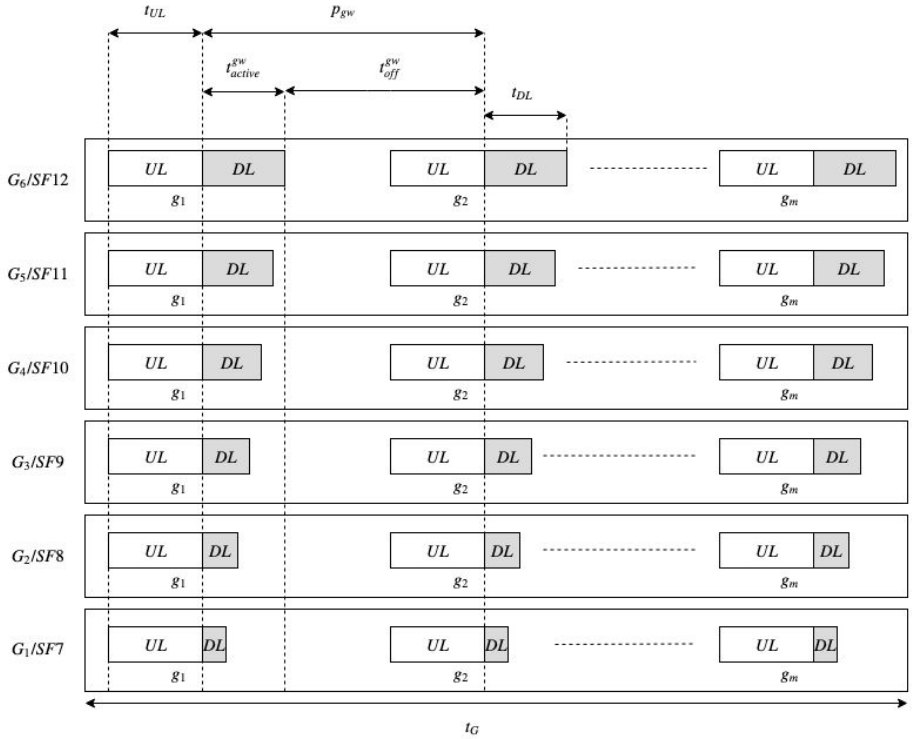

Figure 4.3. System Model

Additionaly, each group starts with UL slots followed by one DL slot of which time-on-air is equal to one UL slot in the group. In addition, there is a constant time, which is the active period of the GW, between the DL slot of each group in a super-group. According to the system model, the system is designed as a periodic two dimension of array, whose rows correspond to the super-groups and columns match to the groups, as shown in Figure 4.3.

Moreover, the groups in each super-group have group ids, and the number of groups in each super-group is the same. The tiime duration of the UL slots in each

Table 4.1. Time definitions in the System Model

Symbol	Description
t_{DL}	Time duration of one slot DL in a group (differs by each super-group)
t_{UL}	Time duration of the entire UL slots in a group (same for each super-group)
t_G	Time duration of the each super group (same for each super-group)
t_{off}^{gw}	Time off duration of gateway "gw" (same for each super-group)
t_{active}^{gw}	Active time duration of gateway "gw" (same for each super-group)
p_{gw}	Transmission period of gateway "gw" (same for each super-group)

group, and the time duration of each super-group are equal. Also, starting transmission time of the groups with the same group id in the different super-groups is the same. Thus, the GW can transmit ACK to each ED inside the groups with the same group id in each super-group at the same time.

4.2.2. System Scheduling

As shown in Figure 4.3, a group consists of two communication partitions. According to Figure 4.4, the UL section is divided into identical time slots, which differ for each super-group. The ED in the group can randomly select a time slot when making a transmission. After transmitting the message, the ED opens its receive window at the DL section of the group. For realizing the system model, the EDs should know the schedule parameters for their group, time slot duration of the group, and first group transmission time in their own super-groups. After getting the schedule parameters from the NS, the ED is synchronized with the system.

After registering to the network, the ED sends a request to NS for getting l_{type}, subscription_id, T_1, and t_G to synchronize itself with the GW according to the system model design in Figure 4.4.

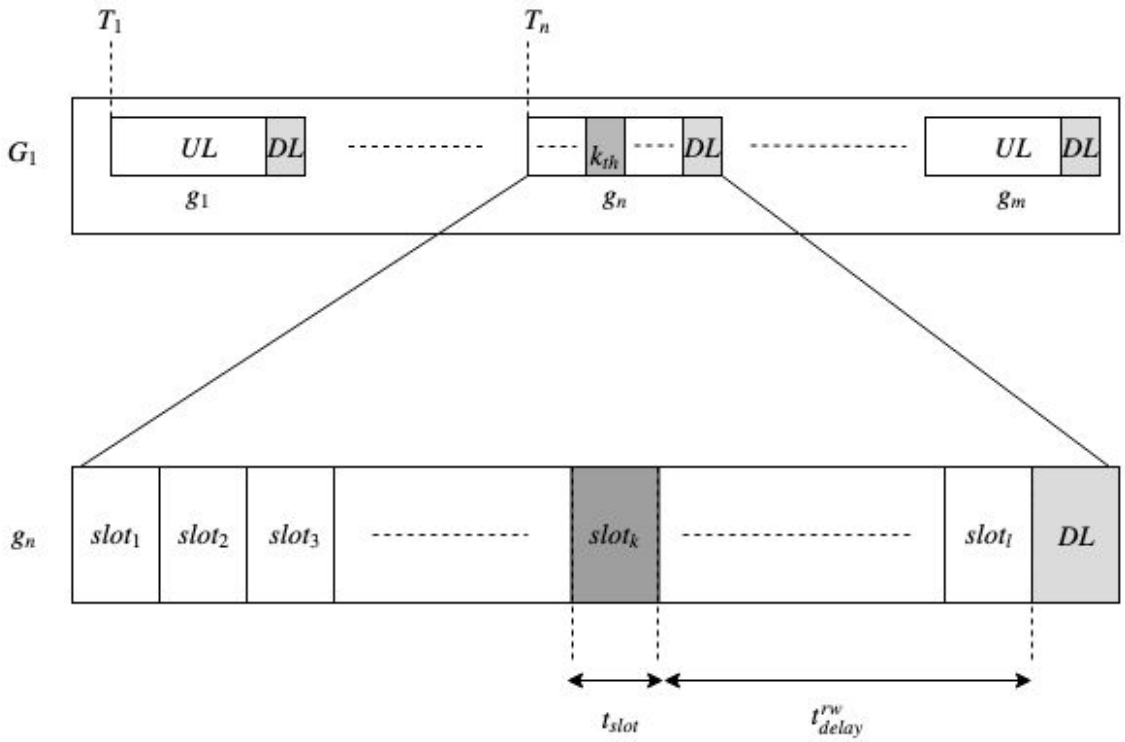

Figure 4.4. ED in g_n, which is a group with the id n of G_1 super-group, transmits a message at $slot_k$. After transmitting the message, ED opens its receive window end of t^{rw}_{delay} time.

Table 4.2. Synchronization parameters received by an ED from the NS

Symbol	Description
subscription_id	Subscription id of the ED (It is used for describing its transmission time and is used to check its) ACK status by controlling the received ACK message.
l_{type}	The payload type used in the network
T_1	The transmission time of the first group in its super-group as shown in Figure 4.4
t_G	Described as in Table 4.1

After getting the parameters in Table 4.2, the ED should calculate own transmission schedule. According to the scenario in Figure 4.4 and the model in Figure 4.3, the ED should consider the steps explained below:

(i) Firstly, ED calculates time-on-air of the t^{gw}_{active} with respect to $G_6/SF12$ super-group and the payload type l_{type} by using Equation 2.3.

(ii) It calculates the GW transmission period p_{gw} as a summation of the t^{gw}_{active} and t^{gw}_{off}, which is evaluated by using Equation 2.7.

(iii) It finds number of groups, m, in the super-group G_1 by

$$m = 2^{\left\lfloor \log_2 \frac{t_G - T_1}{p_{gw}} \right\rfloor}. \tag{4.1}$$

(iv) ED takes $log_2 m$ right-most bit of the subscription_id as the group id. n is found by converting the binary representation of the group id to decimal.

(v) ED calculates T_n, which is the transmission start time of g_n by

$$T_n = T_1 + (n-1) \cdot p_{gw}. \tag{4.2}$$

(vi) It calculates time-on-air of t_{slot} with respect to $G_1/SF7$ super-group and the payload type l_{type} by using Equation 2.3.

(vii) Finally, it transmits on $slot_k$ by choosing slot k randomly in the range of [1, l], after finding the slot number l in the UL section of the group g_n by

$$l = \frac{t_{UL}}{t_{slot}}. \tag{4.3}$$

Table 4.3 shows the calculated schedule parameters for the given synchronization parameters.

Table 4.3. Calculated schedule parameters for $subscription\_id = 10011010110$, $l_{type} = min$, $T_1 = 0s$, and $t_G = 3600s$. The ED is in the $G_1/SF7$ super-group, $DC = 1\%$ and $t_{UL} = 15s$

Symbol	**Value**
t^{gw}_{active}	1.318912s
p_{gw}	131.8912s
m	16
n	6
T_n	659.456s
t_{slot}	0.061696s
l	243
k	10

4.2.3. Aggregated Acknowledgement

After transmitting the message, the ED opens its receive window in the DL section of its group for retrieving the DL message, which is an aggregated ACK message. The GW can create the aggregated ACK message by using a NA or BEA method. After getting the DL message, the ED checks the received aggregated ACK message for subscription_id to find the DL message containing its ACK.

4.2.3.1. Naive Aggregation. In NA, the GW collects subscription_id of the successful transmitters. After collecting subscription_id for all EDs, the GW creates an aggregated

ACK message for the active group in each super-group. The creation of the ACK message is shown with an example in Table 4.4.

Table 4.4. NA example with $m = 8$ (taking right-most 3 bits of the subscription_id, which is 010)

Super-Group	**Successful subscription_id**	**Aggregated ACK**
$G_1/SF7$	1000010, 1100010, 0100010	010100011000100
$G_2/SF8$	1110010, 1101010, 0110010	010111011010110
$G_3/SF9$	1001010, 1111010, 0101010	010100111110101
$G_4/SF10$	1100010, 1110010, 1001010	010110011101001
$G_5/SF11$	0001010, 1010010, 0010010	010100010100010
$G_6/SF12$	1011010, 1110010, 0101010	010101111100101

In Table 4.4, an aggregated ACK starts with the binary notation of the group id, followed by the compressed successful subscription_id of the devices by extracting group id from them.

4.2.3.2. Boolean Expression Aggregation. In BEA, the GW collects subscription_id of the successful transmission devices. After finishing the collection of the ids, the GW creates an aggregated ACK message for the active group in each super-group. The creation of the ACK message is shown with an example in Table 4.5.

In Table 4.5, collected ids are given to Quine McCluskey algorithm to represent them as a boolean expression [32]. The boolean expression format $-100 + 1 - 00$ contains $[-100, 1 - 00]$ as max terms and $+$ as an operator when searching for the boolean expression of the $G_1/SF7$ in Table 4.5. After obtaining the boolean expression, it should be converted to its binary notation through encoding. In the max term, every character exactly matches with the binary, which is created by extracting group id from ubscription_id, such as 1000 for subscription_id 1000010. Furthermore, the max term only consists of $[' -', ' 0', ' 1']$ characters. Binary notations of the characters are $[10, 00, 01]$ so that the max term -100 is encoded as 10010000. Besides, the $+$ operator in the

Table 4.5. BEA example with $m = 8$ (taking right-most 3 bits of the subscription_id, which is 010)

Super-Group	**Successful subscription_id**	**Boolean Expression**	**Aggregated ACK**
$G_1/SF7$	1000010 1100010 0100010	'-100'+ '1-00'	0101001000001100000
$G_2/SF8$	1110010 1101010 0110010	'1101'+ '-110'	0100101000110010100
$G_3/SF9$	1001010 1111010 0101010	'0101'+ '1111'+ '1001'	010000100010101010101000001
$G_4/SF10$	1100010 1110010 1001010	'110-'+ '1-01'	0100101001001100001
$G_5/SF11$	0001010 1010010 0010010	'-010'+ '0001'	0101000010000000001
$G_6/SF12$	1011010 1110010 0101010	'1011'+ '0101'+ '1110'	01001000101000100010101010 0

boolean expression is omitted when encoding the boolean expression, owing to that length of the encoded max term is known. Hence, the encoded boolean expression is shown as 1001000001100000 for the boolean expression $-100 + 1 - 00$.

After getting the encoded version of the boolean expression, group id is added to the begining of the boolean expression. Hence, the aggregated ACK message is created.

On the other hand, if a device does not find its subscription id inside the aggreagated ACK message, then it should retransmit its message in the next super-group iteration to comply with the specifications of LoRaWAN.

4.3. Mathematical Model

Table 4.6. Details of the symbols used in the mathematical model

Symbol	**Value**	**Description**
I	$\{i \mid 1 \leq i \leq m\}$	*Group ids*
J	$\{j \mid 1 \leq j \leq n\}$	*SuperGroup periods*
K	$\{k \mid 7 \leq k \leq 12\}$	*Spreading Factors*
t_{ijk}	$(i \in I,\ j \in J,\ k \in K)$	*Transmission count*
S_k	$(k \in K)$	*Time slot count*
G_{ijk}	$(i \in I,\ j \in J,\ k \in K)$	*Offered load*
P_{ijk}	$(i \in I,\ j \in J,\ k \in K)$	*Probability of success*

In Table 4.6, I is a group id set between the values 1 to m. The maximum group number in all super-groups, m, is calculated by Equation 4.1. J is a period number set between 1 and n. n is related to the super-group duration t_G while the system run time is t_R seconds. If the system is running indefinitely, n converges to infinity. P_{ijk} is equal to mathematical model used for modelling probability of success of time-slotted ALOHA MAC protocol.

$$P_{ijk} = e^{-G_{ijk}} \tag{4.4}$$

The proposed solution is mathematically modeled by Equation 4.4 for showing its probability of success. Moreover, Equation 4.4 is modelled by using Poisson Distribution [33]. The reason for that, A2S2-LoRaWAN uses time slotted ALOHA MAC protocol [34].

Equation 4.5 is used for calculating the offered load. The offered load is used in Equation 4.4. The offered load in Group i of Super-group k during the j_{th} period, G_{ijk}, depends on the current transmission count t_{ijk}, the summation of each failed transmission count until the j_{th} period, and the slot number in any group of super-group k.

$$G_{ijk} = \begin{cases} \frac{\sum_{a=0}^{j-1} \left\{ t_{iak} \cdot \prod_{b=a}^{j-1} (1 - P_{ibk}) \right\} + t_{ijk}}{S_k}, & \text{if } j > 0; \\ \frac{t_{i0k}}{S_k}, & \text{if } j = 0; \end{cases} \tag{4.5}$$

The initial offered load for $j = 0$ is calculated by Equation 4.5. Also, the second offered load depends on the first offered load. The recursive offered load in Equation 4.6 is derived by using Equations 4.5 and 4.4.

$$G_{ijk} = \frac{\sum_{a=0}^{j-1} \left\{ t_{iak} \cdot \prod_{b=a}^{j-1} (1 - P_{ibk}) \right\} + t_{ijk}}{S_k}$$

$$
\begin{aligned}
j = 1; \quad G_{i1k} &= \frac{t_{i0k}.(1 - P_{i0k}) + t_{i1k}}{S_k} \\
S.G_1 &= t_0.(1 - P_0) + t_1 \\
&= [S.G_0].(1 - P_0) + t_1 \\
j = 2; \quad G_{i2k} &= \frac{t_{i0k}.(1 - P_{i0k}).(1 - P_{i1k}) + t_{i1k}.(1 - P_{i1k}) + t_{i2k}}{S_k} \\
S.G_2 &= t_0.(1 - P_0).(1 - P_1) + t_1.(1 - P_1) + t_2 \\
&= [t_0.(1 - P_0) + t_1].(1 - P_1) + t_2 \\
&= [S.G_1].(1 - P_1) + t_2 \\
j = 3; \quad G_3 &= \frac{t_0.(1 - P_0).(1 - P_1).(1 - P_2) + t_1.(1 - P_1).(1 - P_2) + t_2.(1 - P_2) + t_3}{S} \\
S.G_3 &= t_0.(1 - P_0).(1 - P_1).(1 - P_2) + t_1.(1 - P_1).(1 - P_2) + t_2.(1 - P_2) + t_3 \\
&= [t_0.(1 - P_0).(1 - P_1) + t_1.(1 - P_1) + t_2].(1 - P_2) + t_3 \\
&= [S.G_2].(1 - P_2) + t_3 \\
&\cdot \\
&\cdot \\
&\cdot \\
j = j; \quad G_j &= \frac{S.G_{j-1}.(1 - P_{j-1}) + t_j}{S} \\
&= \frac{S.G_{j-1}.(1 - e^{-G_{j-1}}) + t_j}{S} \\
&= \frac{S_k.G_{ij-1k}.(1 - e^{-G_{ij-1k}}) + t_{ijk}}{S_k}
\end{aligned}
$$

$$
\therefore G_{ijk} = G_{ij-1k} \cdot (1 - e^{-G_{ij-1k}}) + \frac{t_{ijk}}{S_k}. \tag{4.6}
$$

5. EXPERIMENTS AND RESULTS

Before presenting the results of the experiments, we give the details of LoRaWAN and A2S2-LoRaWAN simulators. The experiment scenarios are given in the second section.

5.1. Simulators

Understanding the network performance of A2S2-LoRaWAN requires a comparison with the LoRaWAN. The simulators are implemented in Python for realizing the A2S2-LoRaWAN and LoRaWAN. Besides, the mathematical model is implemented in Python to validate the proposed solution. A2S2-LoRaWAN simulator is implemented according to the A2S2-LoRaWAN specification in Chapter 4.

LoRaWAN simulator is implemented according to the LoRaWAN specification. When realizing the LoRaWAN simulator, the following assumptions are considered:

- Communication is on a bidirectional channel for a single GW.
- Retransmissions are implemented.
- The GW transmits ACK messages on the first receive window or the second receive window of the ED.
- Transmitting ACKs has higher priority over other transmissions at the GW.
- ACK transmission is canceled when the GW in time off duration due to the DC restriction.
- A collision in the UL occurs when the same SF EDs overlap in time and space.

5.2. Experiment Scenarios

Experiment scenarios are based on the ED count in the network, payload load types used in the network traffic, and the distributions of SFs for EDs. The ED count in the network directly affects the network capacity; therefore, the ED count is increased

to observe its effects on the network performance. Also, different load types are used in the scenarios to increase the load in the network, time-on-air of the packages, and the number of collisions. Besides, device distributions based on their SFs affect the network traffic [35], so uniform and inverse exponential distributions are used in each experiment scenario. The experiment scenario parameters are summarized in Table 5.1.

Table 5.1. Parameters for each scenario

Input	**Value**
Device count	$\{1000, 2500, 5000, 7500, 10000\}$
Load type	$\{Min, Avg, Max\}$
SF distribution	$\{Uniform, InverseExponential\}$

According to Table 5.1, the load type input values are defined as Min, Avg and Max. The load types differ by SFs; the meaning of the load type for each SF is described in Table 5.2.

Table 5.2. The byte value of Min, Avg, and Max load types for each SF

SpreadingFactors	**Min**	**Avg**	**Max**
SF7	10	125	250
SF8	10	125	250
SF9	10	60	123
SF10	10	30	59
SF11	10	30	59
SF12	10	30	59

Three scenarios are run on A2S2-LoRaWAN simulator, LoRaWAN simulator, and the mathematical Model of the A2S2-LoRaWAN 15 times. The scenario parameters are given in Table 5.3. 5.1.

Table 5.3. Scenarios parameters: DeviceCount, LoadType, and SFDistribution

Scenario	**Inputs**
Increasing device count	DeviceCount=$\{1000, 2500, 5000, 7500, 10000\}$ LoadType=$\{Min\}$ SFDistribution=$\{InverseExponential\}$
Increasing message load	DeviceCount=$\{5000\}$ LoadType=$\{Min, Avg, Max\}$ SFDistribution=$\{InverseExponential\}$
Changing SF distribution	DeviceCount=$\{5000\}$ LoadType=$\{Min, Avg, Max\}$ SFDistribution=$\{Uniform\}$

5.3. Experiment Results

In each experiment scenario, A2S2-LoRaWAN and LoRaWAN simulators run with the same system parameters. The Super-group duration is defined as 3600 seconds, and UL section duration of a group is set to 15 seconds in A2S2-LoRaWAN simulator. On the other hand, other system environment parameters are set as shown in Table 5.4.

Table 5.4. Common system environment parameters for the simulations

Parameter	**Value**
Simulation Runtime	86400 seconds (24 hours)
DC	1%
Network topology	one GW, one channel

A2S2-LoRaWAN performance should be compared with LoRaWAN performance by observing their probability of success during transmission in each scenario. Improvement on UL traffic and DL traffic of A2S2-LoRaWAN should be considered. Also, each

ED in the simulators is forced to transmit one packet during the simulation runtime until reaching the upper bound of the retransmission.

5.3.1. Increasing Device Count

Increasing the transmitter count in the network topology affects the supportable capacity of the network due to the growing number of packet collisions.

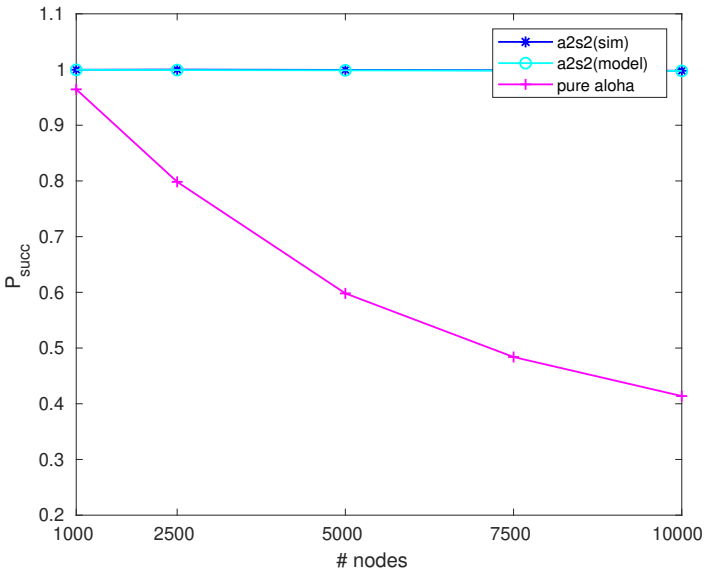

Figure 5.1. The Probability of success of A2S2-LoRaWAN simulation model (a2s2(sim)), A2S2-LoRaWAN mathematical model (a2s2(model)) and LoRaWAN simulation (pure aloha) with respect to the increasing node count in the network. (SFDistribution : $InverseExponential$, LoadType : min)

In Figure 5.1, P_{succ} of the proposed system model is nearly equal to 1 and is not dependent on the increasing node count. Besides, the proposed mathematical model validates the proposed system model results. However, the success rate of LoRaWAN decreases while increasing the transmitter count in the network.

In Figure 5.2, P_{succ} of each super-group in the suggested system model is almost similar to 1 and does not vary with increasing node count. Furthermore, the proposed

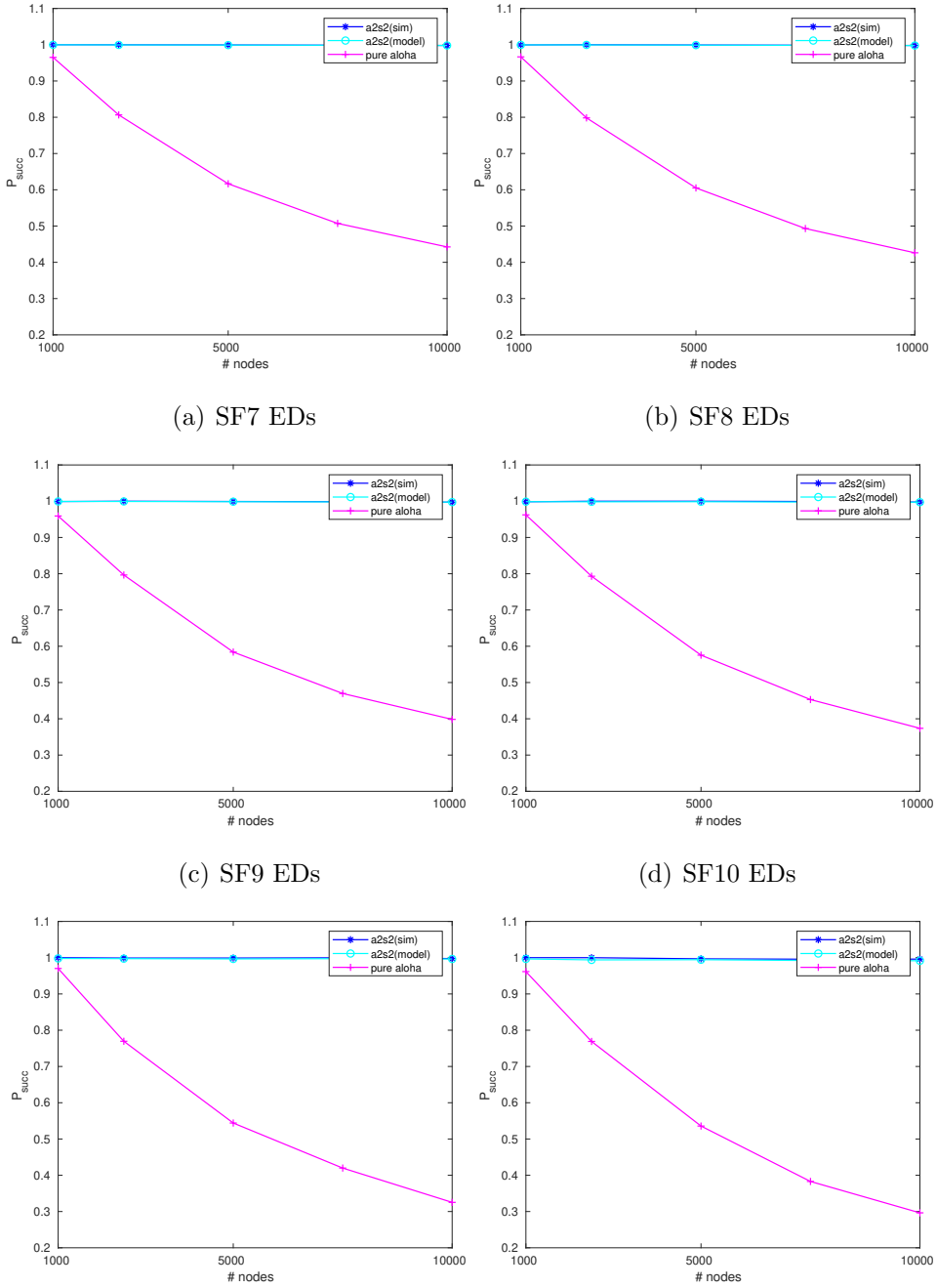

(a) SF7 EDs

(b) SF8 EDs

(c) SF9 EDs

(d) SF10 EDs

(e) SF11 EDs

(f) SF12 EDs

Figure 5.2. The Probability of success of A2S2-LoRaWAN simulation model (a2s2(sim)), A2S2-LoRaWAN mathematical model (a2s2(model)) and LoRaWAN simulation (pure aloha) with respect to the increasing node count and SFs. (SFDistribution : $InverseExponential$, LoadType : min)

mathematical model overlaps with the suggested system model. On the other hand, the success rate of the LoRaWAN drops while the transmitter count in the network grows.

In this scenario, each super-group has 16 groups, and each super-group slot number in the UL section of their groups is different. Moreover, the group slot number of each super-group is decreasing from SF7 to SF12. According to Figure 5.2, the resources in each super-group can handle the load in the executed scenarios, however, LoRaWAN cannot.

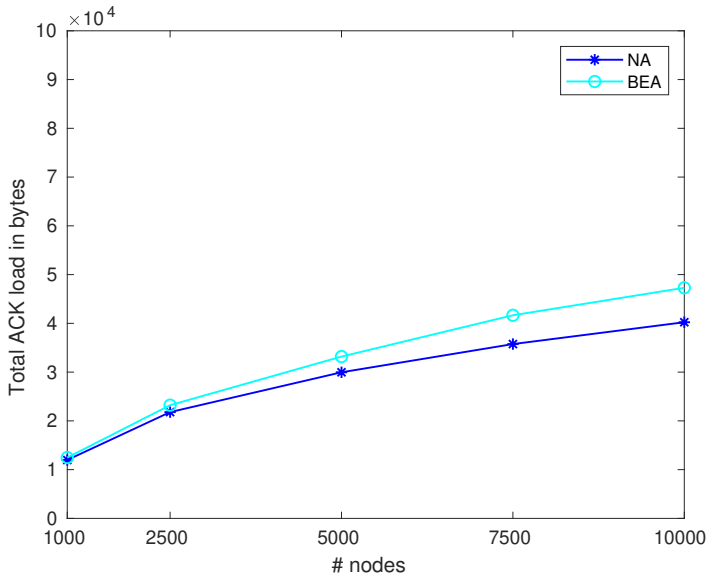

Figure 5.3. Compression ACK message performance of ACK aggregation methods NA and BEA in A2S2-LoRaWAN while increasing the node count in the network. (SFDistribution : $InverseExponential$, LoadType : min)

In Figure 5.3, NA performs better than BEA, and the difference between their produced aggregated message size increases with the growing transmitter count. The reason is that BEA method does not give efficient results when running with sparse subscription id list. In this case, although the ED number in the group is rising, the group number in the super-group is not changed. Hence, the numerical distance between the subscription ids of successful EDs could be increasing. So, BEA method could not work well with sparse subscription id list of successful EDs.

Table 5.5 shows that retransmissions for each device count in LoRaWAN is bigger than A2S2-LoRaWAN's. This is due to the fact that packet collisions occur more

Table 5.5. UL and DL performance of A2S2-LoRaWAN and LoRaWAN. $DevNm$ shows device number in the network. $ULMsgNm$ and $DLMsgNm$ show the total number of transmitted messages in UL and DL. (SFDistribution : $InverseExponential$, LoadType : min)

DevNm	**A2S2 UL-DL**		**LoRaWAN UL-DL**	
	ULMsgNm	**DLMsgNm**	**ULMsgNm**	**DLMsgNm**
1000	1004	863	1345	964
2500	2521	1484	5947	1995
5000	5100	1872	18122	2990
7500	7740	2101	32149	3629
10000	10440	2135	46573	4138

frequently in LoRaWAN, compared to A2S2-LoRaWAN.

5.3.2. Increasing Message Load

Increasing message load results in increments at traffic load in the network, time-on-air of the packages, and packet collision in the network.

In Figure 5.4, P_{succ} of the proposed system model is nearly equal to 1 when the load type is Min or Avg. However, when the load type is Max, P_{succ} of the proposed system model closes to 0.97. In addition, the offered mathematical model verifies the proposed system model results. Although changes in load type affect the proposed model negatively, the success rate of the LoRaWAN conserves its state, because the number of groups inside the super-groups decreases from 16 to eight when the load type is the maximum. So, the traffic load of the groups in each super-group increases in the maximum load type.

In Figure 5.5, P_{succ} of each super-group in the proposed system model is essentially close to 1 except for SF7 and SF8 super-groups. One of the reasons is that SF of

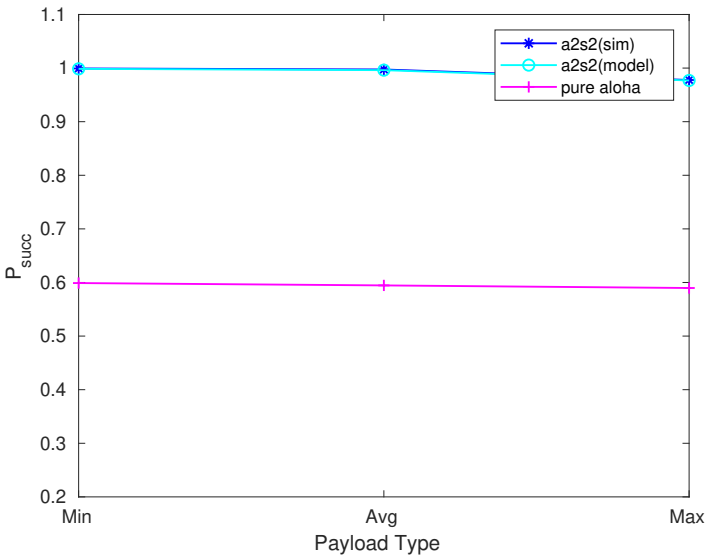

Figure 5.4. The Probability of success of A2S2-LoRaWAN simulation model (a2s2(sim)), A2S2-LoRaWAN mathematical model (a2s2(model)) and LoRaWAN simulation (pure aloha) with respect to the increasing sent message size in the network. (SFDistribution : $InverseExponential$, DeviceCount : 5000)

EDs is distributed inverse-exponentially from SF7 to SF12. Decreasing of the group number in super-group negatively affects SF7 and SF8 more than other super-groups. Therefore, the increase in their traffic loads is more than the other super-groups. Also, the proposed mathematical model confirms the proposed system model results.

In Figure 5.6, NA performs better than BEA, and the difference between their produced aggregated message size does not change through increased message load. However, after using Max payload type in the network, there is a similar decrease observed in the size of the ACK messages produced by the two methods due to the decrease in the number of groups in the super-groups.

In Table 5.6, increase in the load types decreases UL message count in LoRaWAN because time-on-air of the messages increases. However, the total network load rises. In A2S2-LoRaWAN, retransmissions grow on the UL. At Max load type, although

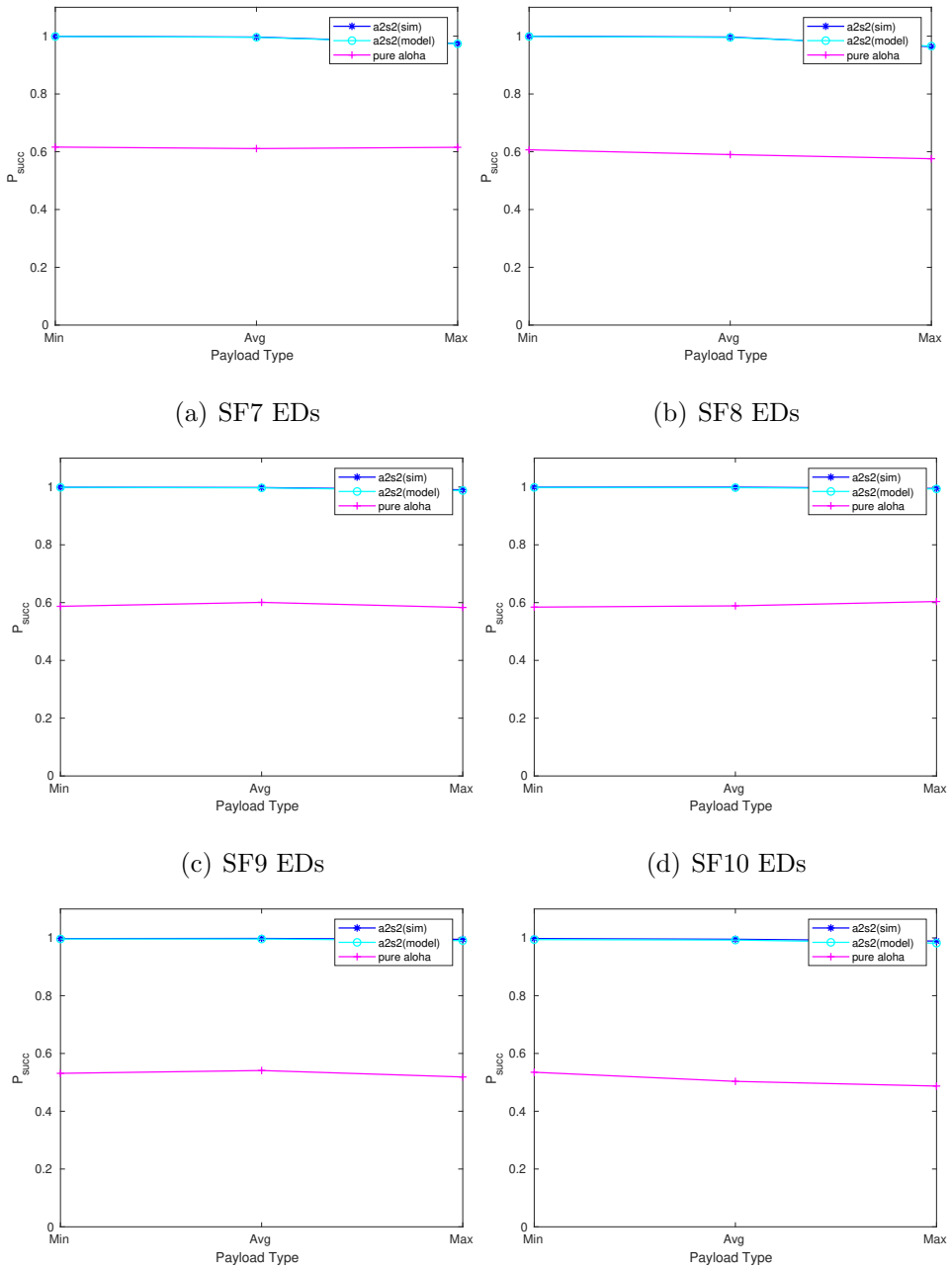

(a) SF7 EDs

(b) SF8 EDs

(c) SF9 EDs

(d) SF10 EDs

(e) SF11 EDs

(f) SF12 EDs

Figure 5.5. The Probability of success of A2S2-LoRaWAN simulation model (a2s2(sim)), A2S2-LoRaWAN mathematical model (a2s2(model)) and LoRaWAN simulation (pure aloha) with respect to the increasing sent message size and SFs.(SFDistribution : *InverseExponential*, DeviceCount : 5000)

P_{succ} of each load type is nearly equal, there is an enormous decrease in DL message counts due to the decrease in the number of groups in each super-group. Also, there is

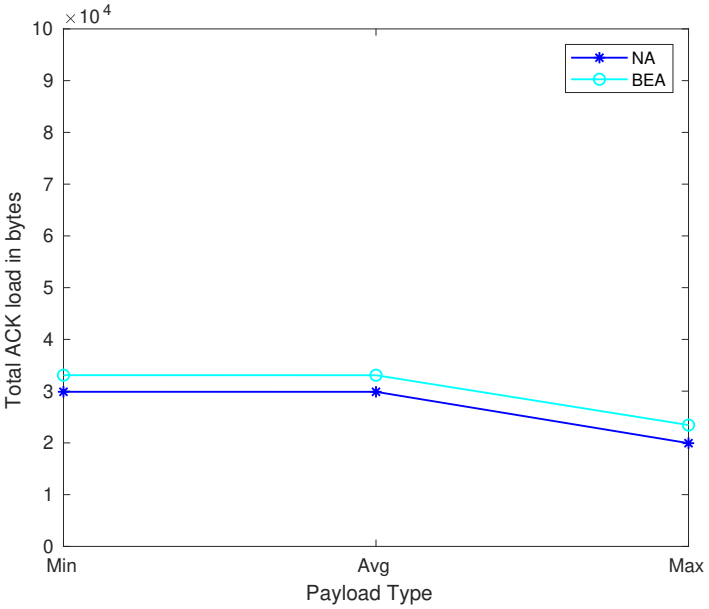

Figure 5.6. Compression ACK message performance of ACK aggregation methods NA and BEA in A2S2-LoRaWAN while increasing sent message size in the network.(SFDistribution : $InverseExponential$, DeviceCount : 5000)

Table 5.6. UL and DL performance of A2S2-LoRaWAN and LoRaWAN. $DevNm$ shows device number in the network. $ULMsgNm$ and $DLMsgNm$ show the total number of transmitted messages in UL and DL. (SFDistribution : $InverseExponential$, DeviceCount : 5000)

LoadType	**A2S2 UL-DL**		**LoRaWAN UL-DL**	
	ULMsgNm	**DLMsgNm**	**ULMsgNm**	**DLMsgNm**
Min	5093	1865	18090	2994
Avg	5318	1866	17063	2972
Max	7230	1064	16354	2948

an increase in UL message traffic due to the increased packet collisions.

5.3.3. Changing SF Distribution

SF distribution types affect each super-group network load and device count. Changing the distribution from inverse exponential to uniform could affect each super-group negatively or positively. Here, the test scenario differs from the case in Section 5.3.2 only in the distribution type; we change it from nverse exponential to uniform distribution. Therefore, the count of SF12 and SF11 EDs is growing, and the count of SF7 and SF8 EDs is decreasing.

In Figure 5.7, P_{succ} of a2s2(sim)-ud is lower than P_{succ} of a2s2(sim)-iexd when the payload type is Max. Besides, P_{succ} of pure aloha-ud is lower than P_{succ} of pure aloha-iexd because time-on-air of the transmitted messages is increasing. Therefore, retransmissions and collisions are rising.

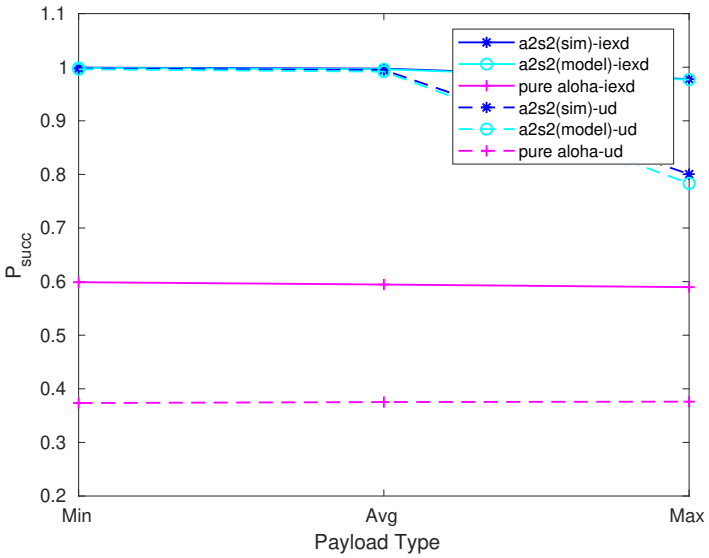

Figure 5.7. The Probability of success of A2S2-LoRaWAN simulation model with inverse exponential/uniform SF distribution (a2s2(sim)-iexd/ud), A2S2-LoRaWAN mathematical model with inverse exponential/uniform SF distribution (a2s2(model)-iexd/ud) and LoRaWAN simulation with inverse exponential/uniform SF distribution (pure aloha-iexd/ud) with respect to the increasing sent message size in the network. (DeviceCount : 5000)

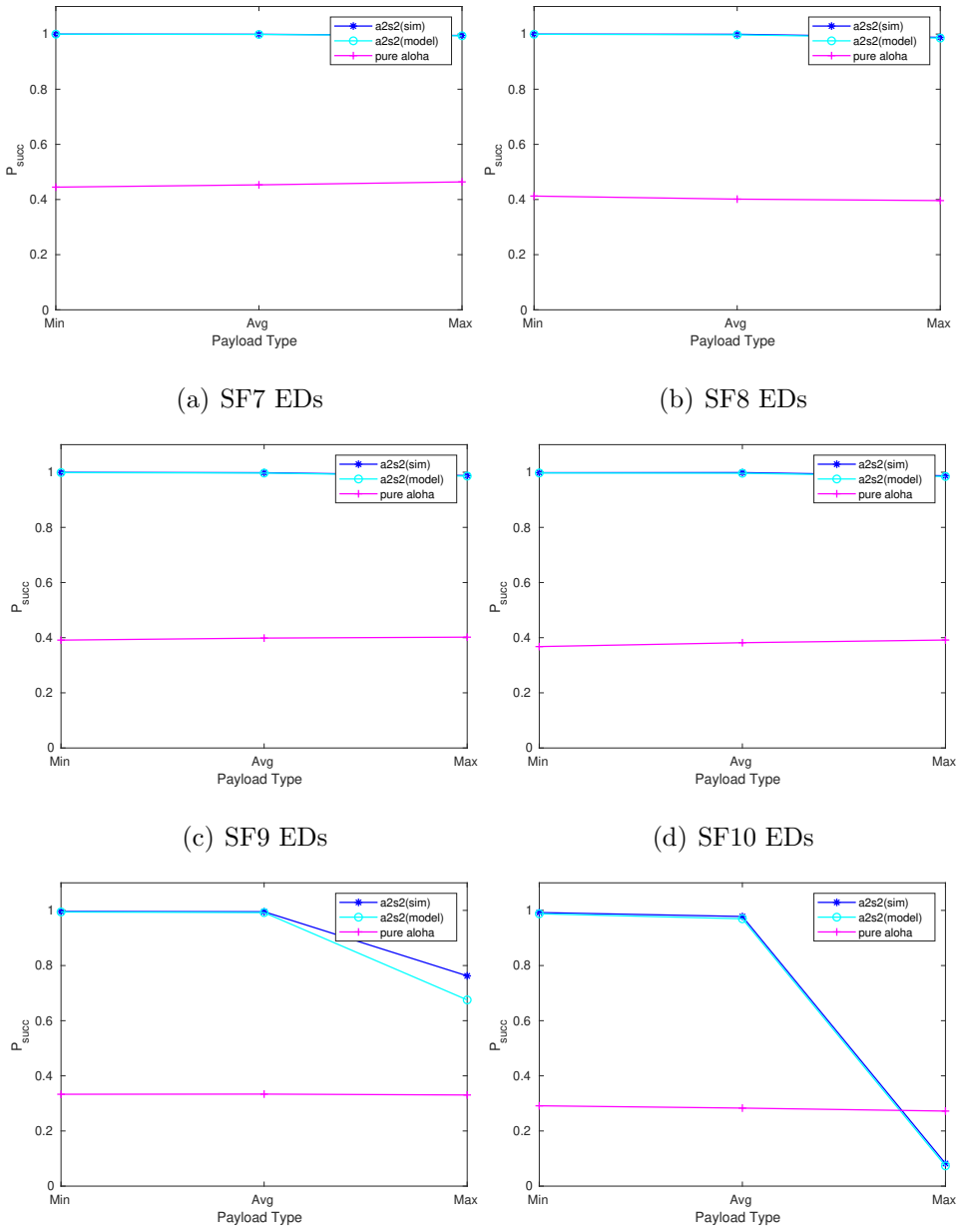

(a) SF7 EDs

(b) SF8 EDs

(c) SF9 EDs

(d) SF10 EDs

(e) SF11 EDs

(f) SF12 EDs

Figure 5.8. The Probability of success of A2S2-LoRaWAN simulation model (a2s2(sim)), A2S2-LoRaWAN mathematical model (a2s2(model)) and LoRaWAN simulation (pure aloha) with respect to the increasing sent message size and SFs. (SFDistribution : $Uniform$, DeviceCount : 5000)

In the case of Figure 5.8, ED counts of SF11 and SF12 are increasing, and ED counts of SF7 and SF8 are decreasing against the ED count in the case of Figure 5.5. As a result, P_{succ} of SF11 and SF12 super-groups is decreasing against P_{succ} of Figure 5.5 for A2S2-LoRaWAN at Max load type. On the other hand, the success rate of the super-groups, which contains SF7 or SF8 EDS, is increasing. Besides, the mathematical model validates the observed results. The reason is that the number of slots in the group of each super-group is not changed although ED count changes. Therefore, the offered load in SF7 and SF8 super-groups is decreasing. However, the offered load is rising for SF11 and SF12 super-groups.

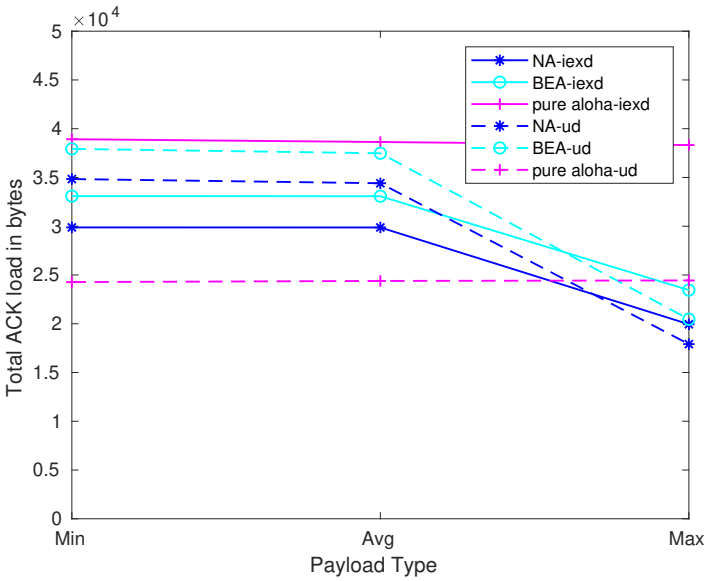

Figure 5.9. Compression ACK message performance of ACK aggregation methods NA (NA-iex/ud) and BEA (BEA-iex/ud), and ACK message performance of LoRaWAN (pure aloha-iexd/ud) while increasing sent message size in the network. (DeviceCount : 5000)

In Figure 5.9, the gap between the values of NA-ud and BEA-ud is almost equal to the difference between values of NA-iexd and BEA-iexd. On the other hand, the sizes of ACKs produced by NA-ud and BEA-ud pass shown values of NA-iexd and BEA-iexd at Min and Avg payloads. The reason is that the collisions at SF11 and SF12 are increasing, so the number of successful transmitters per ACK message in NA-ud and BEA-ud is lower than the number of successful transmitters per ACK message

NA-iexd and BEA-iexd. On the other hand, P_{succ} of a2s2(sim)-ud (Figure 5.8) is nearly equal to P_{succ} of a2s2(sim)-iexd (Figure 5.8). Therefore, the GW sends more aggregated ACK than the GW in the case of Figure 5.6. In addition to the comparison, the total ACK loads of NA-ud and BEA-ud is lower than the values of NA-iexd and BEA-iexd at Max payload. The reason is that collisions at Max payload exceed collisions at other payload types. Therefore, the number of aggregated ACKs sent by the GW in NA-ud and BEA-ud case is lower than the number of ACKs in the case of NA-iexd and BEA-iexd.

Table 5.7. UL and DL performance of A2S2-LoRaWAN and LoRaWAN. $DevNm$ shows device number in the network. $ULMsgNm$ and $DLMsgNm$ show the total number of transmitted messages in UL and DL. (SFDistribution : $Uniform$, DeviceCount : 5000)

LoadType	**A2S2 UL-DL**		**LoRaWAN UL-DL**	
	ULMsgNm	**DLMsgNm**	**ULMsgNm**	**DLMsgNm**
Min	5280	2248	23093	1867
Avg	5581	2216	21847	1876
Max	11796	992	20686	1880

In Table 5.7, there is a UL-DL performance comparison of A2S2-LoRaWAN and LoRaWAN with respect to load type of messages. In A2S2-LoRaWAN, there is a slightly increasing in $ULMsgNm$ and decreasing in $DLMsgNm$ when changing load type from Min to Avg. However, sharply increase in $ULMsgNm$ and decrease in $DLMsgNm$ is observed when changing load type from Avg to Max. The reason is the increasing collissions, so retransmissions at Max load type are greater than retransmissions at other load types. In LoRaWAN, there is a slight decrease on $ULMsgNm$ from Min load type to Max load type since the total time-off duration of the EDs in LoRaWAN is increasing. Therefore, the frequency of retransmissions is decreasing. On the other hand, $DLMsgNm$ remains almost the same. Besides, each SF distribution affects the results in Table 5.7 and Table 5.6 in different ways. In A2S2-LoRaWAN, collisions in SF11 and SF12 super-groups are more than the collisions in the case of

Table 5.6. Therefore, the sum of $ULMsgNm$ is larger than the sum of $ULMsgNm$ in Table 5.6. In addition to $ULMsgNm$, $DLMsgNm$ at Min and Avg is larger than $DLMsgNm$ in Table 5.6. The reason is that P_{succ} of the two cases is almost same althougth collisions in the case of Table 5.7 are more than collisions in the case of Table 5.6. Therefore, the GW sends much more ACKs than the case of Table 5.6.

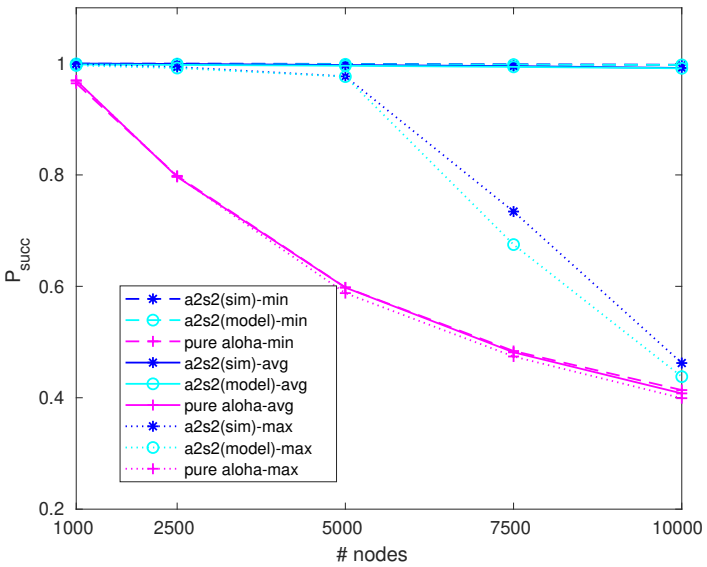

Figure 5.10. The Probability of success of A2S2-LoRaWAN simulation model (a2s2(sim)), A2S2-LoRaWAN mathematical model (a2s2(model)) and LoRaWAN simulation (pure aloha) with respect to the increasing node count in the network and increasing sent message size in the network. (SFDistribution : $InverseExponential$)

In Figure 5.10, there are four critical points where the number of nodes is 1000, 5000, 7500, and 10000. All observations are almost equal to each other at 1000 nodes. After, the decrease in pure aloha-min/avg/max is seen inverse exponentially through the increase in the node count. Also, pure aloha is not adversely affected by the change of the message load, compared to a2s2, since pure aloha does not work on the time-slotted frame structure. Another side, there is a moment of break between a2s2(sim/model)-min/avg and a2s2(sim/model)-max at 5000 nodes. The groups in a2s2-min/avg handle the load through the increase in the node count, so P_{succ} values of them are nearly equal to one. However, after the breaking event at 5000 nodes, a2s2-max can not handle the traffic load because of the fact that the number of a2s2-

max groups in its super-groups is lower than the number of a2s2-min/avg groups in their super-groups. Besides, the number of time slots in a2s2-max groups is lower than the number of time slots in a2s2-min/avg groups. On the other hand, the differences between P_{succ} values of a2s2-max(sim) and a2s2-max(model) at 7500 nodes and 10000 nodes are 0.05 and 0.03. The reason is that a2s2-max(sim) drops transmitters reaching the retransmission upper bound (eight transmission per message), however a2s2-max(model) does not. Therefore, the collisions in a2s2-max(model) are more than the collisions in a2s2-max(sim). Finally, at 10000 nodes, a2s2-min/avg have best success rates, and pure aloha-min/avg/max is worst.

To sum up, we perform simulations to compare the network performance of A2S2-LoRaWAN and LoRaWAN. According to the results, a GW in A2S2-LoRaWAN can work with 10.000 EDs at Min payload type with almost 100% success rate. However, A GW in LoRaWAN can work with 1.000 EDs. While A2S2-LoRaWAN decreases UL-DL traffic five times compared to LoRaWAN, its success rate of it with 10.000 EDs at Min payload type is twice better than the success rate of LoRaWAN. On the other hand, A2S2-LoRaWAN is sensitive to the change of the payload type since the number of slots in the groups depends on the payload type. However, it still performs better than LoRaWAN. When SF distribution changes from inverse-exponential to uniform, A2S2-LoRaWAN shows lower performance for SF12 EDs; still, it has a better performance than LoRaWAN. Besides, inverse-exponential distribution of SFs on EDs is expected for LoRaWAN [35]. Moreover, the NA method shows better performance than the BEA method for each case. Thus, A2S2-LoRaWAN generally has better performance on scalability and UL-DL traffic than LoRaWAN.

6. CONCLUSION

In the thesis, the pure ALOHA-type MAC protocol used in LoRaWAN prevents the scaling of the network. Therefore, we introduce a scheduling method for LoRaWAN called A2S2-LoRaWAN for improving the scalability of LoRaWAN. After implementing the simulation of A2S2-LoRaWAN and LoRaWAN, specific experiment scenarios are run on the simulators to analyze the effects of A2S2-LoRaWAN and LoRaWAN on the network scalability, and DL and UL traffic.

According to the experiment results, there is a decrease in DL and UL traffic when using A2S2-LoRaWAN instead of LoRaWAN. Besides, A2S2-LoRaWAN is more scalable than LoRaWAN. In addition, NA is better than BEA.

As the future work, multi GW scenarios can be also included into the problem for improving the solution. Traffic types or application content types can be considered for improving the solution. Moreover, A2S2-LoRaWAN solution can be added to NetworkSimulator-3 as a module. Retransmission limit in LoRaWAN can be added to A2S2-LoRaWAN Mathematical Model as a constraint. Lastly, energy consumption performance of A2S2-LoRaWAN should be investigated.

REFERENCES

1. Gubbi, J., R. Buyya, S. Marusic and M. Palaniswami, "Internet of Things (IoT): A vision, architectural elements, and future directions", *Future generation computer systems*, Vol. 29, No. 7, pp. 1645–1660, 2013.

2. Cisco, V., "Cisco Visual Networking Index: Forecast and Trends, 2017–2022", *White Paper*, 2018.

3. Rose, K., S. Eldridge and L. Chapin, "The internet of things: An overview", *The Internet Society (ISOC)*, pp. 1–50, 2015.

4. Ray, P. P., "A survey on Internet of Things architectures", *Journal of King Saud University-Computer and Information Sciences*, Vol. 30, No. 3, pp. 291–319, 2018.

5. Gazis, V., M. Goertz, M. Huber, A. Leonardi, K. Mathioudakis, A. Wiesmaier and F. Zeiger, "Short paper: IoT: Challenges, projects, architectures", *2015 18th International Conference on Intelligence in Next Generation Networks*, pp. 145–147, IEEE, 2015.

6. Raza, U., P. Kulkarni and M. Sooriyabandara, "Low power wide area networks: An overview", *IEEE Communications Surveys & Tutorials*, Vol. 19, No. 2, pp. 855–873, 2017.

7. Compatibility, E. and R. S. Matters, "Short Range Devices (SRD); Radio Equipment to Be Used in the 25 MHz to 1000 MHz Frequency Range With Power Levels Ranging Up to 500 mW", *ETSI EN*, Vol. 330, pp. 220–1, 2012.

8. Reynders, B., W. Meert and S. Pollin, "Range and coexistence analysis of long range unlicensed communication", *2016 23rd International Conference on Telecommunications (ICT)*, pp. 1–6, IEEE, 2016.

9. Sanchez-Iborra, R. and M.-D. Cano, "State of the art in LP-WAN solutions for industrial IoT services", *Sensors*, Vol. 16, No. 5, p. 708, 2016.

10. Finnegan, J. and S. Brown, "A comparative survey of LPWA networking", *arXiv preprint arXiv:1802.04222*, 2018.

11. de Carvalho Silva, J., J. J. Rodrigues, A. M. Alberti, P. Solic and A. L. Aquino, "LoRaWAN—A low power WAN protocol for Internet of Things: A review and opportunities", *2017 2nd International Multidisciplinary Conference on Computer and Energy Science (SpliTech)*, pp. 1–6, IEEE, 2017.

12. Bankov, D., E. Khorov and A. Lyakhov, "On the limits of LoRaWAN channel access", *2016 International Conference on Engineering and Telecommunication (EnT)*, pp. 10–14, IEEE, 2016.

13. San, C., J. Bergs, C. Hawinkel and J. Famaey, "Comparison of Lo RaWAN classes and their power consumption", *IEEE Symposium on Communications and Vehicular Technology*, pp. 8–13, 2017.

14. Adelantado, F., X. Vilajosana, P. Tuset-Peiro, B. Martinez, J. Melia-Segui and T. Watteyne, "Understanding the limits of LoRaWAN", *IEEE Communications magazine*, Vol. 55, No. 9, pp. 34–40, 2017.

15. Knight, M. and B. Seeber, "Decoding LoRa: Realizing a Modern LPWAN with SDR", *Proceedings of the GNU Radio Conference*, Vol. 1, No. 1, 2016, `https://pubs.gnuradio.org/index.php/grcon/article/view/8`.

16. Bor, M. C., J. Vidler and U. Roedig, "LoRa for the Internet of Things.", *EWSN*, Vol. 16, pp. 361–366, 2016.

17. Reynders, B. and S. Pollin, "Chirp spread spectrum as a modulation technique for long range communication", *2016 Symposium on Communications and Vehicular Technologies (SCVT)*, pp. 1–5, IEEE, 2016.

18. Augustin, A., J. Yi, T. Clausen and W. Townsley, "A study of LoRa: Long range & low power networks for the internet of things", *Sensors*, Vol. 16, No. 9, p. 1466, 2016.

19. Masoudi, M., A. Azari, E. A. Yavuz and C. Cavdar, "Grant-free radio access IoT networks: Scalability analysis in coexistence scenarios", *2018 IEEE International Conference on Communications (ICC)*, pp. 1–7, IEEE, 2018.

20. Marais, J. M., R. Malekian and A. M. Abu-Mahfouz, "LoRa and LoRaWAN testbeds: A review", *2017 Ieee Africon*, pp. 1496–1501, IEEE, 2017.

21. Alliance, L., "LoRaWAN™ 1.1 Specification", *technical specification*, 2017.

22. Alliance, L., "LoRaWAN™ 1.1 Regional Parameters", *technical specification*, 2017.

23. Ortín, J., M. Cesana and A. Redondi, "How do ALOHA and Listen Before Talk Coexist in LoRaWAN?", *2018 IEEE 29th Annual International Symposium on Personal, Indoor and Mobile Radio Communications (PIMRC)*, pp. 1–7, IEEE, 2018.

24. Pop, A.-I., U. Raza, P. Kulkarni and M. Sooriyabandara, "Does bidirectional traffic do more harm than good in LoRaWAN based LPWA networks?", *GLOBECOM 2017-2017 IEEE Global Communications Conference*, pp. 1–6, IEEE, 2017.

25. Mikhaylov, K., J. Petäjäjärvi and A. Pouttu, "Effect of Downlink Traffic on Performance of LoRaWAN LPWA Networks: Empirical Study", *2018 IEEE 29th Annual International Symposium on Personal, Indoor and Mobile Radio Communications (PIMRC)*, pp. 1–6, IEEE, 2018.

26. Capuzzo, M., D. Magrin and A. Zanella, "Confirmed traffic in LoRaWAN: Pitfalls and countermeasures", *2018 17th Annual Mediterranean Ad Hoc Networking Workshop (Med-Hoc-Net)*, pp. 1–7, IEEE, 2018.

27. Reynders, B., Q. Wang, P. Tuset-Peiro, X. Vilajosana and S. Pollin, "Improving reliability and scalability of lorawans through lightweight scheduling", *IEEE Internet of Things Journal*, Vol. 5, No. 3, pp. 1830–1842, 2018.

28. Haxhibeqiri, J., I. Moerman and J. Hoebeke, "Low overhead scheduling of lora transmissions for improved scalability", *IEEE Internet of Things Journal*, 2018.

29. Zorbas, D., K. Q. Abdefadeel, V. Cionca, D. Pesch and B. O'Flynn, "Offline scheduling algorithms for time-slotted lora-based bulk data transmission", *the IEEE 5th World Forum on Internet of Things (WF-IoT). IEEE*, pp. 1–6, 2019.

30. Bankov, D., E. Khorov and A. Lyakhov, "Mathematical model of LoRaWAN channel access", *2017 IEEE 18th International Symposium on A World of Wireless, Mobile and Multimedia Networks (WoWMoM)*, pp. 1–3, IEEE, 2017.

31. Capuzzo, M., D. Magrin and A. Zanella, "Mathematical Modeling of LoRa WAN Performance with Bi-directional Traffic", *2018 IEEE Global Communications Conference (GLOBECOM)*, pp. 206–212, IEEE, 2018.

32. Jain, T. K., D. S. Kushwaha and A. K. Misra, "Optimization of the quine-mccluskey method for the minimization of the boolean expressions", *Fourth International Conference on Autonomic and Autonomous Systems (ICAS'08)*, pp. 165–168, IEEE, 2008.

33. Ferre, G., "Collision and packet loss analysis in a LoRaWAN network", *2017 25th European Signal Processing Conference (EUSIPCO)*, pp. 2586–2590, IEEE, 2017.

34. Polonelli, T., D. Brunelli and L. Benini, "Slotted ALOHA Overlay on LoRaWAN-A Distributed Synchronization Approach", *2018 IEEE 16th International Conference on Embedded and Ubiquitous Computing (EUC)*, pp. 129–132, IEEE, 2018.

35. Mikhaylov, K., J. Petaejaejaervi and T. Haenninen, "Analysis of capacity and scalability of the LoRa low power wide area network technology", *European Wireless*

2016; 22th European Wireless Conference, pp. 1–6, VDE, 2016.